IAEA-TECDOC-717

Guidelines for safe design of shipping packages against brittle fracture

INTERNATIONAL ATOMIC ENERGY AGENCY IAEA

August 1993

FOREWORD

In 1992, the ninth meeting of the Standing Advisory Group on the Safe Transport of Radioactive Materials recommended the publication of this TECDOC in an effort to promote the widest debate on the criteria for the brittle fracture safe design of transport packages. The published IAEA advice on the influence of brittle fracture on material integrity is contained in Appendix IX of the Advisory Material for the IAEA Regulations for the Safe Transport of Radioactive Material (1985 Edition, as amended 1990), Safety Series No. 37. This guidance is limited in scope, dealing only with ferritic steels in general terms. It is becoming more common for designers to specify materials other than austenitic stainless steel for packaging components. The data on ferritic steels cannot be assumed to apply to other metals, hence the need for further guidance on the development of relationships describing material properties at low temperatures.

The methods described in this TECDOC will be considered by the Revision Panel for inclusion in the 1996 Edition of the IAEA Regulations for the Safe Transport of Radioactive Material and the supporting documents. If accepted by the Revision Panel, this advice will be a candidate for upgrading to a Safety Practice. In the interim period, this TECDOC offers provisional advice on brittle fracture evaluation. It is acknowledged that, at this stage, the views expressed do not necessarily reflect those of the governments of Member States or organizations under whose auspices this manuscript was produced.

CONTENTS

Chapter 1
INTRODUCTION

Two paragraphs of the 1985 Edition of IAEA Safety Series No. 6, the Regulations for the Safe Transport of Radioactive Material (as amended 1990), infer the need for acceptable material properties at low temperatures, specifically at -40°C. These are para. 528 — a Type A requirement which also has to be met by Type B designs — and para. 556 — a Type B requirement applying only to Type B packages. The associated guidance information in the 1985 Edition of IAEA Safety Series No. 37, Advisory Material for the IAEA Regulations for the Safe Transport of Radioactive Material (as amended 1990), is essentially contained in Appendix IX, Influence of Brittle Fracture on Material Integrity. Appendix IX is however limited in that it deals only with ferritic steels and then only in general terms. It relies heavily on the extensive database of these materials' low temperature properties which have been compiled since World War II, beginning with the 'Liberty Ship' problems.

It is becoming more common for designers to specify materials other than austenitic stainless steel for nuclear packaging components. Such materials include ductile iron, alloy steel, titanium, depleted uranium, aluminum and borated stainless steel. All of these metals can exhibit non-ductile failure at sufficiently low temperature and at stresses below the yield strength of the material, and specifically when flaws are present. The data on ferritic steels associated with low temperature properties cannot be assumed to apply to other metals and therefore the necessary relationships will have to be developed. To this end it was realized that further guidance to applicants/designers would be required and that revision of Appendix IX of Safety Series No. 37 was therefore necessary.

Methods are described in this TECDOC which may be used by applicants/designers to demonstrate to competent authorities that the materials chosen will maintain the package integrity at low temperatures with respect to shielding, containment, and subcriticality requirements. More precisely, it details methods that can be used to technically justify the design depending upon the amount of materials data available, and specifies varying degrees of conservatism to be applied to these data to give assurance that failure will be prevented.

The effort to revise IAEA Safety Series No. 37 began with a US Department of Transportation (DOT) proposal to the IAEA Continuous Review Committee, in June 1989, to incorporate criteria in Safety Series No. 37 to evaluate brittle fracture of nuclear material transportation packages. The Continuous Review Committee accepted the US proposal. At the 8th meeting of SAGSTRAM, in December 1990, the Science and Technology Agency of Japan further proposed to convene a no-cost Consultants Services Meeting (CSM) in order to write the brittle fracture evaluation criteria. SAGSTRAM provided the IAEA with five specific objectives for the CSM to address:

(1) Review the paper by Sorenson, et al.: "A Proposal for an International Brittle Fracture Acceptance Criterion for Nuclear Material Transport Cask Applications".

(2) Consider all packaging materials with brittle fracture characteristics.

(3) Address issues of "catastrophic flaw, failure prediction, and NDE methods for significant flaws".

(4) Prepare proposed advisory material for inclusion in Safety Series No. 37.

(5) Submit a Consultants Report to the IAEA.

The CSM convened on 9–11 October 1991 and wrote a draft revision to Appendix IX of Safety Series No. 37. The draft Appendix IX, Influence of Brittle Fracture on Material Integrity, was given to CSM delegates to distribute among their own experts for a ninety day review. Comments from this review were then collated and evaluated at a second CSM, convened on 1–3 April 1992.

During the ninety day comment period, CSM members were also given writing assignments that form the basis of this TECDOC. The assignments were collated in February 1992 and reviewed as a whole by the CSM members prior to the second meeting.

The second CSM focused on agreement of the final version of the draft Appendix IX to Safety Series No. 37 and improvements to this TECDOC. The draft Appendix, renamed "Guidelines for Safe Design of Shipping Packages against Brittle Fracture", will be considered by the Revision Panel for inclusion in the 1996 revision of the Regulations and supporting documents. The TECDOC, which was agreed upon during the third CSM, convened on 21–22 October 1992, offers provisional guidance to applicants/designers on brittle fracture evaluation in the interim period. If the draft Appendix is accepted by the Revision Panel, consideration must be given to upgrading this TECDOC to a Safety Practice. In the interim, Chapter 2 of this TECDOC contains the draft Appendix IX to Safety Series No. 37 in its entirety. The numbering system chosen in Chapter 2 is appropriate to draft Appendix IX of Safety Series No. 37. Chapters 3 to 7 provide technical justification for elements of the provisional guidance detailed in Chapter 2.

Chapter 2

DRAFT APPENDIX IX OF SAFETY SERIES No. 37: "GUIDELINES FOR SAFE DESIGN OF SHIPPING PACKAGES AGAINST BRITTLE FRACTURE"

This appendix provides guidance for evaluation of brittle fracture of structural components in radioactive materials (RAM) transport packages. Two basic methods are discussed:

(i) Evaluation of ferritic steels using Charpy or nil-ductility transition temperature measurements correlated to fracture resistance; and

(ii) Assessment of fracture resistance based on a linear-elastic fracture mechanics design evaluation.

The first method is addressed to provide consistency with generally accepted practice for evaluating ferritic steels. The second method, which accounts for the majority of guidance in this appendix, provides a methodology for evaluating brittle fracture that is suitable to a wide range of structural materials. This guidance does not preclude alternative methods that are properly justified by the package designer and accepted by the competent authority.

Many materials are known to be less ductile at low temperatures and high loading rates than at moderate temperatures and static loading conditions. For example, the ability of ferritic steels to absorb energy increases markedly over a narrow temperature range. The highest temperature at which complete brittle fracture occurs for ferritic steels is defined as the nil-ductility transition temperature (NDTT). Similar behaviour is exhibited by other materials, such as ductile iron (DI), some aluminium alloys, and many plastics and elastomers. Loading of these materials under low-ductility conditions can lead to unstable crack propagation with subsequent brittle fracture, even when the nominal stresses are less than the material yield strength. Small crack-like defects in the material may be sufficient to initiate this unstable growth.

One mechanical property that characterizes a material's resistance to crack initiation is its initiation fracture toughness. Measurements of this property, as a function of temperature and loading rate, trace out the transition from brittle to ductile material behaviour. This property is the parameter which quantifies a material's ability to resist crack initiation given a set of known loads (mechanical and environmental) in the presence of crack-like defects. Depending upon the localized state of stress around the defect, and the extent of any plasticity, the parameter is referred to as the stress intensity factor (K_I), if the stress-strain conditions are linear-elastic; or, if the stress-strain conditions are elastic-plastic, the parameter is represented by the energy line integral, J_I. According to fundamental fracture mechanics theory, the applied stress intensity factor (K_I) or the energy line integral (J_I) must be less than the material's fracture toughness ($K_{I(material)}$) or ($J_{I(material)}$) to preclude crack initiation and subsequent brittle fracture (or ductile tearing in the case of elastic-plastic conditions). The particular value of $K_{I\,(material)}$ or $J_{I\,(material)}$ that is acceptable for defining crack initiation depends on loading and environmental combinations of interest. For plane strain conditions the critical fracture toughness is termed K_{Ic} or J_{Ic}. Further, depending upon the loading rate, the linear-elastic parameter is categorized as static (K_{Ic}) or dynamic (K_{Id}) fracture toughness. If the initial depth of the defect, in combination with the applied loading, results in an applied

stress intensity factor that equals the material toughness, crack initiation is imminent and the depth of the defect is referred to as the critical flaw depth. Under increased loading the crack may propagate, leading to flaw instability and failure.

For conservatism, the recommended approach for the evaluation of the potential for brittle fracture of transportation package designs should be based on the **prevention of crack initiation**. The principles of linear-elastic fracture mechanics will normally be appropriate. Under some conditions, and as justified by the package designer and accepted by the competent authority, the principles of elastic-plastic fracture mechanics may be appropriate. In such cases, the prevention of crack initiation remains the governing criterion. Guidance is provided in the following paragraphs for design against crack initiation in packages subjected to the mechanical tests prescribed in paras 622, 625 or 627 of Safety Series No. 6.

The fundamental linear-elastic fracture mechanics equation describes structural behaviour as a function of applied stress and flaw depth:

$$K_I = C\sigma\sqrt{\pi a}, \tag{IX.1}$$

where

K_I = applied stress intensity factor (MPa $\sqrt{m}$);
C = constant based on flaw size, orientation and geometry of the structure;
σ = applied nominal tensile stress (MPa); and
a = flaw depth (m).

Further, to preclude brittle fracture, the applied stress intensity factor should satisfy the relationship

$$K_I < K_{I(material)}, \tag{IX.2}$$

where $K_{I(material)}$ defines the fracture toughness. Where

$$K_I = K_{I(material)}, \tag{IX.3}$$

Eq. (IX.1) can be combined with Eq. (IX.3) to give an expression for the critical flaw depth, a_{cr}, as

$$a_{cr} = \frac{1}{\pi}\left(\frac{K_{I(material)}}{C\sigma}\right)^2. \tag{IX.4}$$

The purpose of the brittle fracture evaluation process is to ensure that the three parameters of this characterization (material fracture toughness, applied stress, and flaw size) satisfy Eqs (IX.1) and (IX.2), thereby precluding crack initiation.

Evaluation methods

Criteria for the prevention of crack initiation and potentially unstable crack propagation in ferritic steel components, such as pressure vessels and piping used in the power, petroleum, and chemical process industries, are well developed, and have been codified into standard practice by a number of national and international standard-writing bodies. These criteria can be classified into two general types: (1) those based solely on material testing requirements, usually intended to demonstrate that some material property (e.g., impact energy) may be correlated to fracture toughness to provide adequate margin against brittle fracture; or (2) those based on a combination of material testing, calculation of applied stresses, and workmanship/inspection standards, intended to demonstrate that sufficient margin exists between the calculated design state and the measured material response state. Method 2 follows the basic fracture mechanics approach described in Eqs (IX.1)–(IX.4). Other evaluation methods are possible. Any approach suggested by the package designer is subject to the approval of the competent authority.

Examples of the first method include the British Standards Institution BS 5500 [1], and the ASME Sections III [2] and VIII [3]. These methods address, for example, ferritic steels with substantial databases which relate impact energy (Charpy testing) to fracture toughness. In such cases, the Charpy impact energy can be used as an indirect indicator of material toughness. This approach may be used for a variety of high quality carbon and carbon-manganese ferritic steels. The basic acceptance criterion for BS 5500 and the two ASME Code documents is the requirement of a minimum impact energy (or lateral expansion) from a Charpy V-notch test at a prescribed temperature.

Another example of the first method is the US Nuclear Regulatory Commission (NRC) regulatory guide, "Fracture Toughness Criteria for Ferritic Steel Shipping Cask Containment Vessels with a Wall Thickness Greater Than Four Inches (0.1 m)", Reg. Guide 7.12 [4]. This criterion **prescribes levels of NDTT** which must be achieved for ferritic steels, based on section thickness and temperature. IT requires a minimum temperature difference between the NDTT of the material and its lowest service temperature, as a function of section thickness. This temperature difference is based on correlations between NDTT and fracture toughness. While this regulatory guide specifically addresses ferritic steels, the same approach could be considered for other materials for which a correlation between NDTT and fracture resistance can be demonstrated. A practical problem in using this approach for other materials is that the standardized test procedure ASTM A208 is valid for ferritic steels only. There are no standardized test methods for measuring the NDTT of other materials.

For the nuclear transportation industry, two significant drawbacks are apparent in the first method: (1) it relies solely on material properties to the exclusion of the designer's ability to limit stresses through provision of impact-limiting devices and non-destructive examination (NDE) sufficient to detect and size prescribed flaws, and (2) the correlation of impact energy to fracture toughness is not applicable to a broad range of materials, thereby restricting the designer's use of alternative containment boundary materials.

Numerous examples of the second method that are valid for nuclear power plant components can be identified. Such examples, although not directly applicable to transport package design evaluation, may be instructive in terms of their use of linear-elastic fracture mechanics principles. These examples include Appendix G of ASME Section III [5]; RCCM Appendix ZG of the French Nuclear Construction Code [6]; MITI Notification 501 from

Japan [7]; the German nuclear design code KTA 3201.2 [8]; the British Standards Institution document PD 6493:1991 [9]; and the Confederation of Independent States (CIS) document [10]. These examples allow the designer the latitude of material selection together with the ability to determine stresses and NDE requirements such that crack initiation and brittle fracture is precluded. The fundamental linear-elastic fracture mechanics approach is applied in all of these cases, although differences arise in the application of safety factors.

Safety factors

Any safety factors that might be applied to Eq. (IX.2), or to the parameters that make up Eq. (IX.2), must account for uncertainties in the calculation or measurement of these parameters. These uncertainties might include those associated with the calculation of the state of stress in the package, the examination of this package for defects, and the measurement of material fracture toughness. In particular, concern about uncertainty in non-destructive examination (NDE) can be accommodated by appropriate conservatism in the selection of the reference flaw.

For the purposes of crack initiation prevention in transport package materials, the safety factors for normal conditions of transport and hypothetical accident conditions should be in general agreement with safety factors that have been developed for similar loading conditions in the referenced applications of the linear-elastic fracture mechanics approach. For example, for loading conditions that are expected to occur during the service life of the package, such as the normal conditions of transport, a safety factor of approximately 3 could be applied to Eq. (IX.2). For unexpected (but design basis) loading conditions, such as the hypothetical accident conditions, a safety factor of approximately 1.4 could be applied to Eq. (IX.2). It should be noted that this safety factor to Eq. (IX.2) can be applied to either the applied stress, σ, or to $K_{I(material)}$. Therefore, this factor of safety can be interpreted as accounting for uncertainty in the calculation of the stress state, or uncertainty in the measurements of $K_{I(material)}$, or as a combination of the two. The factor of safety may be selected and justified by the package designer, with acceptance by the competent authority.

Evaluation procedure

With the safety factors established, the general steps to be followed in order to apply the recommended approach are: (1) postulation of a reference, or design basis, flaw at the most critical location in the packaging, and in the most critical orientation; (2) calculation of the stresses due to the mechanical tests described in paras 622, 625 and 627 of IAEA Safety Series No. 6, ensuring that any required load combinations are considered; (3) calculation of the applied stress intensity factor at the tip of the design basis flaw; (4) determination of the fracture toughness material property; and (5) satisfaction of any margin of safety between this applied stress intensity factor and the accepted material fracture toughness value. This will assure that the flaw will not initiate as a result of the free drop and puncture tests, and therefore will not lead to unstable crack propagation and/or brittle fracture.

A variation on this sequence is for the mechanical tests to be used to demonstrate the resistance to brittle fracture directly. In this case, the test measurements may be used for either, or both, of two purposes — to provide inference of the stress field for applied stress intensity factor calculations, or to provide direct confirmation of the recommended margin against crack initiation. For the second of these, a crack must be placed in the prototype test packaging location most vulnerable to flaw initiation from the mechanical test loads. The

reference flaw shape shall be semi-elliptical, with an aspect ratio (length to depth) of 6:1, or greater. The tip of this artificial flaw should be as crack-like as possible, with a reference flaw acuity that is justified by the package designer and accepted by the competent authority. An acuity of the radius at the extreme tip of the crack of not greater than 0.1 mm has been suggested for ductile iron [11]. The depth of this flaw is determined by using stresses as previously calculated or inferred from strain measurements, and an appropriate factor of safety must also be considered when computing the artificial flaw depth.

Recommendations for each of these procedural steps are provided in the following paragraphs.

Flaw consideration: With respect to either demonstration by analysis or demonstration by test, the reference flaw shall be placed at the surface of the packaging containment wall at the location of the highest applied stress. Where the location of the highest applied stress is uncertain, multiple demonstrations may be required. The orientation of the reference flaw shall be such that the highest tensile component of surface stress, as determined from calculations or experimental measurements, is normal to the plane of the flaw. The depth of the reference flaw shall be such that its relationship to volumetric examination sensitivity, detection uncertainty, rejection flaw size, and critical flaw size is justified. The reference flaw depth should be such that, in association with the demonstrated volumetric and surface examination sensitivity, the non-detection probability is assured to be sufficiently small, as justified by the package designer. A smaller depth may be chosen where the probability of non-detection can be demonstrated to be statistically insignificant.

The reference flaw of 6:1 aspect ratio should have an area, normal to the direction of maximum stress, greater than typical pre-service inspection indications that might be cause of rejection or repair of a fabricated packaging containment wall. However, since the reference flaw is a crack-like surface defect, rather than a more typical real defect (e.g., subsurface porosity cloud or slag inclusion), the selection of this flaw size is extremely conservative relative to workmanship standards.

Fracture toughness considerations: The calculated applied stress intensity factor shall be shown to be less than the material fracture toughness value in Eq. (IX.2), as reduced by the factor of safety. The method for determining the material fracture toughness shall be selected from three options, all of which are illustrated in Fig. 2.1. Each of these options includes the generation of a statistically significant database of material fracture toughness values obtained on product forms that are representative of material suppliers and package applications. The first two options shall include material fracture toughness values that are representative of the strain rate, temperature and constraint conditions (e.g., thickness) of the actual package application. These same considerations apply to material fracture toughness measurements used to support an elastic-plastic fracture evaluation.

Option 1 shall be based on the determination of a minimum value of fracture toughness at a temperature of -40°C for a specific material. The minimum value is shown in Fig. 2.1 as representing a statistically significant data set, for a limited number of heats from a limited number of material suppliers, obtained at appropriate loading rate and geometric constraint conditions. The heats shall be representative of product forms appropriate for the particular package application.

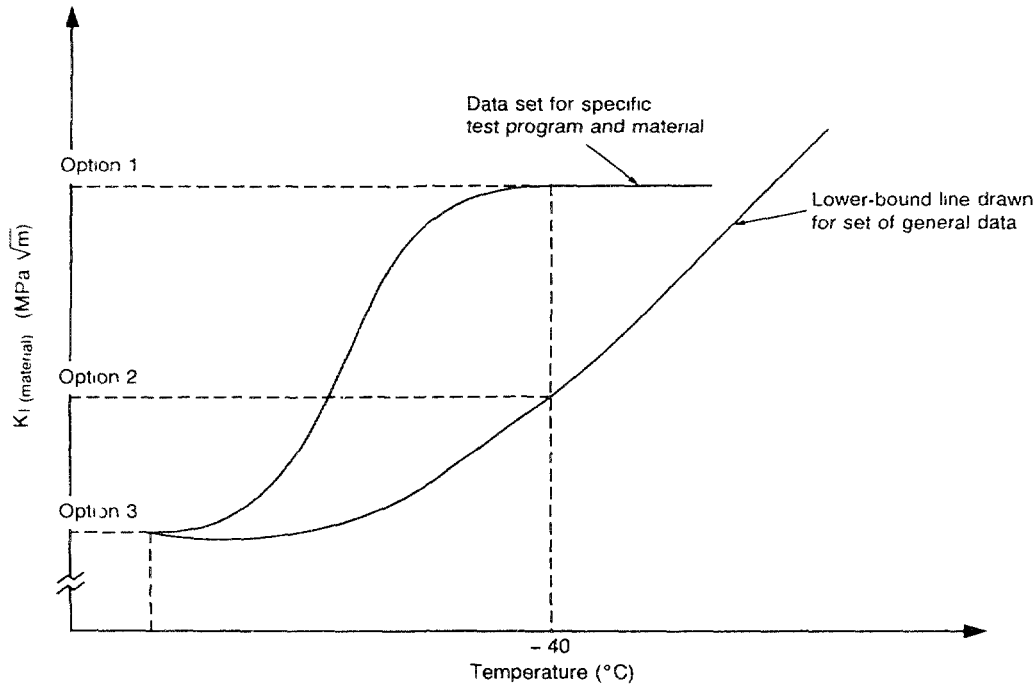

FIG. 2.1. Relative values of $K_{I\,(material)}$ measurements based on the selection of options 1, 2 or 3.

Option 2 shall be based on the determination of a lower-bound or near lower-bound value of material fracture toughness, $K_{I(material)} = K_{Ib}$, as shown in Fig. 2.1. This option would encompass the reference material fracture toughness determination for ferritic steels that is prescribed, for example, in the ASME Code Section III, Appendix G [5]. The lower-bound or near lower-bound value can be based on a composite of static, dynamic, and crack arrest fracture toughness data. An advantage of this option is the potential for reducing the testing programme for materials that can be referenced to the lower-bound or near lower-bound curve. A relatively small, but suitable, number of data points may be sufficient to demonstrate the applicability of the curve to specific heats, grades or types of material.

Option 3 shall be based on the minimum value of a statistically significant fracture toughness data set satisfying the static loading rate and crack tip constraint requirements of ASTM E399 [12]. The test temperature shall be at least as low as -40°C, but may have to be reduced even lower to satisfy the ASTM E399 conditions, as shown in Fig. 2.1. The conservatism of this option may be such that, as justified by the package designer and accepted by the competent authority, a reduced factor of safety could be used.

Stress consideration: With respect to either demonstration by test or analysis, the calculation of the applied stress intensity factor at the tip of the reference flaw shall be based on maximum tensile stresses that are justified by the package designer and accepted by the Competent Authority. The stresses may be determined by calculations for an unflawed package. When the stress field is inferred from surface strain measurements or either a scale - model or full-scale package performance test, the inferred stress field shall also be justified. The applied stress intensity factor may be calculated directly from stress analysis or conservatively calculated from handbook formulas that account for flaw shape and other geometric and material factors.

Since the calculated stress fields may be dependent on impact limiter performance, mass distributions and structural characteristics of the package itself, the justification of the stresses will in turn depend on the justification of analytical models. The justification of stress fields inferred from performance tests will depend on the justification of test instrumentation characteristics, locations and data interpretation. Evaluation of either calculated or inferred stress fields may also involve an understanding of relevant dynamic material and structural characteristics.

References

[1] BRITISH STANDARDS INSTITUTION, Specification for Unfired Fusion Welded Pressure Vessels, BS 5500, BSI, London (1991).

[2] AMERICAN SOCIETY OF MECHANICAL ENGINEERS, Boiler and Pressure Vessel Code, Section III, Division 1, Rules for the Construction of Nuclear Power Plant Components, ASME, New York (1992).

[3] AMERICAN SOCIETY OF MECHANICAL ENGINEERS, Boiler and Pressure Vessel Code, Section VIII, Division 1, Rules for Construction of Pressure Vessels, ASME, New York (1992).

[4] NUCLEAR REGULATORY COMMISSION, Fracture Toughness Criteria for Ferritic Steel Shipping Cask Containment Vessels with a Wall Thickness Greater Than Four Inches (0.1 m), Regulatory Guide 7.12, NRC, Washington, DC (1991).

[5] AMERICAN SOCIETY OF MECHANICAL ENGINEERS, Boiler and Pressure Vessel Code, Section III, Division 1 — Appendices, Appendix G: Protection Against Nonductile Failure, ASME, New York (1992).

[6] French Nuclear Construction Code; RCCM: Design and Construction Rules for Mechanical Components of PWR Nuclear Islands, Subsection Z, Appendix ZG, Fast Fracture Resistance (1985).

[7] JAPANESE MINISTRY FOR INTERNATIONAL TRADE AND INDUSTRY, Technical Criteria for Nuclear Power Structure, Notification No. 501.

[8] Sicherheitstechnische Regel des KTA, Komponenten des Primaerkreises von Leichtwasserreaktoren; Teil 2: Auslegung, Konstruktion und Berechnung, KTA 3201.2, Fassung 3/84, Bundesanzeiger, Bonn (1985).

[9] BRITISH STANDARDS INSTITUTION, Guidance on Methods for Assessing the Acceptability of Flaws in Fusion Welded Structures, PD 6493, BSI, London (1991).

[10] Gosstandart, Determination of Fracture Toughness Characteristics Under Static Loading, GOST 25.506-85 (1985); and Determination of Fracture Toughness Characteristics Under Dynamic Loading, RD-50-344-8 (1983).

[11] CENTRAL RESEARCH INSTITUTE OF ELECTRIC POWER INDUSTRY, Research on Quality Assurance of Ductile Cast Iron Casks, EL 87001, CRIEPI, Tokyo (1988).

[12] AMERICAN SOCIETY FOR TESTING AND MATERIALS, Annual Book of ASTM Standards: Standard Test Method for Plane-Strain Fracture Toughness of Metallic Materials, Volume 03.01, ASTM E399-83, Philadelphia, PA (1983).

Chapter 3

JUSTIFICATION OF THE CRACK INITIATION METHODOLOGY

The fundamental engineering discipline that defines the ability of material to resist crack initiation and subsequent crack growth is fracture mechanics. As with most physical phenomena, fracture mechanics is a large field of study and is therefore divided into subsets based on material response to mechanical and environmental loadings. A material's response to such loadings can be characterized as either linear-elastic or elastic-plastic. These two responses are a function of material properties and section design. In general, many materials with, for example, a body centred cubic or hexagonal close packed atomic structure have the potential to fail in a brittle manner (i.e. linear-elastic response). Further, the thickness of the material influences its response; as constraint in the section increases, the potential for brittle fracture increases.

Fracture mechanics design can also be based on either crack initiation or crack arrest. The crack initiation criterion precludes any crack initiation resulting from applied stresses. The crack arrest criterion allows crack initiation, but asserts that any growth of the crack will arrest prior to catastrophic collapse of the structural component. Fracture mechanics guidance in Chapter 2 of this document is based on linear-elastic behaviour and the crack initiation criterion. This approach results in the maximum conservatism in evaluating the brittle fracture potential in package designs. In addition, this approach avoids the need to deal with uncertainty in the calculation or measurement of crack growth. The justification for this approach will follow after a brief historical review of the development of the field of fracture mechanics.

The development in the field of fracture mechanics technology can be divided into three stages. The first stage spans the period from 1913 to 1947, during which the predominant mechanical representation of brittle fracture was one published by Griffith in 1920. This theory was based, in part, on analytical results published by Inglis in 1913.

The second stage of development covers the period from 1947 to 1965, the year the American Society for Testing and Materials (ASTM) Committee E24 on Fracture Testing was established. This stage in the development of fracture mechanics can be subdivided into two periods. The first 12 years, 1947 to 1959, represent the period during which fracture mechanics technology was developed under the leadership of G.R. Irwin and was applied to the design of engineering structures. Irwin recognized that most of the analytical methods needed to formulate the mechanics of fracture on a sound technical basis were available. The second period, 1959 to 1965, is marked by the formation of an ASTM Special Technical Committee. This committee studied the various methodologies that were available to analyse fracture and adopted the fracture mechanics technology developed by Irwin. This recognized the engineering significance of the technical development and facilitated its use and further developments. Essentially, the ASTM Special Committee accepted a leadership role in extending the development of fracture mechanics. Between 1960 and 1965, the application of this technology was extended to the study of fatigue crack growth, stress corrosion cracking, and elastic-plastic fracture. First reports issued by the Special Technical Committee in 1960 contributed significantly to the acceptance and to the advancement of fracture mechanics technology.

The third stage in the progression of fracture mechanics technology started with the formation of Committee E24 on Fracture Testing in 1965 and continues to the present time. The formation of this committee provided a forum for the development and application of this technology by many scientists and engineers in the United States and around the world.

Engineering applications of fracture mechanics have matured and become essential over the years. Initial fracture mechanics awareness grew out of the fracture failures in some of the USA World War II 'Liberty Ships'. More sophisticated applications were then identified with the aircraft industry and extended to other applications such as heavy rotating components of large steam turbine electric generators.

As the necessity of this engineering discipline has grown and been accepted by industry, consensus codes and standards have been developed in order to assure consistent application of the methodology. ASTM provides the authoritative test procedures for measuring fracture toughness of material specimens and there are numerous design codes throughout the world that embrace fracture mechanics criteria for evaluating brittle fracture.

Applying fracture mechanics criteria for the evaluation of brittle fracture in structural components of RAM transport packages is a logical extension of the fracture mechanics methodology. Clearly, these criteria must assure both the user and the regulator that the approach can assure that brittle fracture will not occur and that there is a reasonable level of conservatism in the design.

Linear-elastic fracture mechanics and the crack initiation criterion were selected as the basis for the draft Appendix IX guidance because these approaches result in conservative designs that provide significant margin against brittle failure. Linear-elastic fracture mechanics represent complete brittle behaviour of a structural material subjected to mechanical and environmental loadings. In reality, candidate structural materials for RAM packages exhibit, at worst, a mixed-mode behaviour (e.g. partial brittle fracture and partial ductile tearing), and often exhibit a completely ductile response. A ductile material mitigates stress concentrations through yielding and redistribution of the applied stresses over a larger area. Applying the linear-elastic criterion to elastic-plastic materials requires the conversion of an elastic-plastic measurement, J_{Ic}, to the linear-elastic K_{Ic}. This is a conservative conversion as long as the loadings do not result in through-wall yielding (a condition that is not permissible by standard structural criteria). The effect of the conversion acts to reduce the allowable flaw size in the structural component and thereby increases the safety of the design.

Selection of the crack initiation criterion has a strong institutional basis. Conducting a certification test that results in crack initiation and subsequent crack growth with eventual arrest may be arguable on a technical basis, but does not provide a great degree of confidence for the general public. Assurance that a crack will not even initiate provides a much better safety argument than to argue that a crack may initiate and grow, but that it will arrest before catastrophic failure occurs.

Crack initiation is also conservative because the dynamic effects associated with crack arrest are much more pronounced. For a typical package, hypothetical accident conditions result in peak loadings over a time frame of approximately 20 milliseconds. Although this time may seem short, it is a rather long load duration and material properties do not differ much from static conditions. For a crack arrest criterion, a propagating crack travels at approximately the speed of sound. Material properties do change at these very high strain rates and, in general, exhibit more linear-elastic (i.e., brittle) behaviour as rates increase.

Failure assessment diagrams are one way to relate mechanics of material's failure theory with fracture mechanics failure theory. The ordinate in Fig. 3.1(a) tracks tensile stress and assumes failure occurs at an applied tensile stress equivalent to the yield stress of the material. The abscissa tracks the stress intensity factor, K_I, and assumes failure occurs when K_I reaches the material's fracture toughness value, K_{Ic}. The quadrant drawn from 1.0 on the ordinate to 1.0 on the abscissa represents the boundary of failure. Designs falling within the quadrant would not fail from either excessive tensile strain or from an excessive stress intensity factor. Since the assumptions that ductile rupture occurs at stresses equal to the yield strength and brittle fracture occurs at stress intensity factors equal to crack initiation toughness are very conservative relative to actual failure points, this failure boundary is understated.

Results of actual drop test programmes are plotted in Fig. 3.1. Data from the Sandia National Laboratories MOSAIK Drop Test Program [3.1], the German Bundesanstalt fuer Materialforschung und -pruefung (BAM) VHLW Drop Test Program [3.2] and the Japanese Central Research Institute of Electric Power Industry (CRIEPI) [3.3] full-scale drop test programme relate test results to the failure boundary. These drop test programmes demonstrated the integrity of monolithic ductile iron packages subjected to Type B accident condition testing.

Figure 3.1(b) represents a failure assessment diagram with safety factors introduced. For hypothetical accident conditions, regulations allow stresses to exceed the yield strength. The NRC, for example, allows the applied stress to reach 1.6 times the yield strength. If the ductile rupture failure point corresponds to the ultimate strength of the material, 1.6 times the yield strength corresponds to a safety factor of between 1.25 and 1.5, depending upon whether the material is ferritic or austenitic. For the brittle fracture axis, a safety factor of 1.4 (or a safety coefficient of 0.7) has been applied to the stress intensity factor. This acts to change the failure boundary from a quadrant to an approximate quarter-ellipse. Visually, it is shown that a higher degree of conservatism is placed on the stress intensity factor than on the applied stress. This is appropriate since characterization of fracture toughness properties and analysis of stress intensity factors is less refined than characterizing material tensile properties and analyzing applied stresses. Given this example of applying safety factors to the design, four of the seven plotted drop test results represent designs that would not have satisfied acceptance criteria. However, since the package did not fail in any of the drop tests, the conservatism of the crack initiation criterion is demonstrated.

In reality, the failure boundaries shown in Fig. 3.1 do not look exactly as shown. A precise description corresponding to Fig. 3.1 is discussed in the R6 method issued by Nuclear Electric plc (formerly the Central Electricity Generating Board) in the United Kingdom. These diagrams provide a useful visualization to the pacakage designer and the competent authority of the interaction of applied stress and applied stress intensity factor relative to the allowables on one graph.

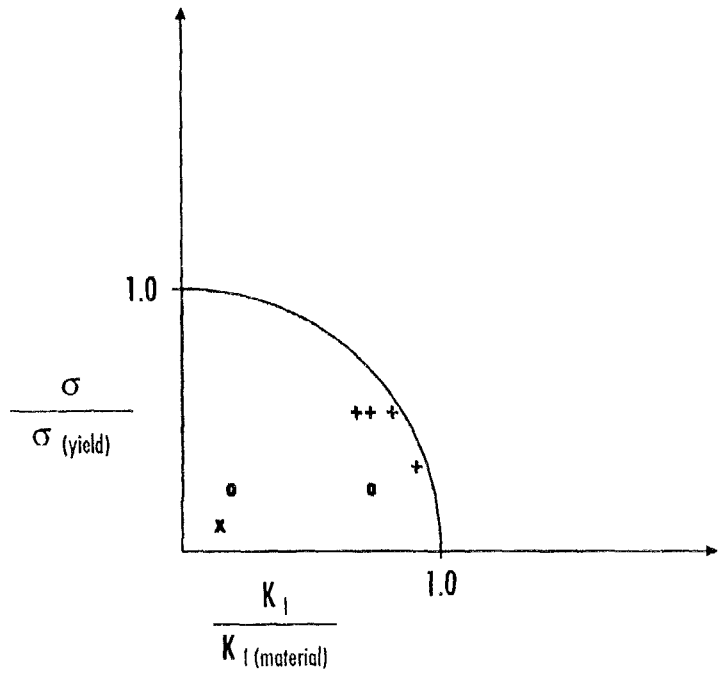

+ Results of four cask drop tests conducted at SNL
x Result of one cask drop test conducted at BAM
o Results of two cask drop tests conducted at CRIEPI

Note: Crack initiation did not occur in any of these drop tests.

(a)

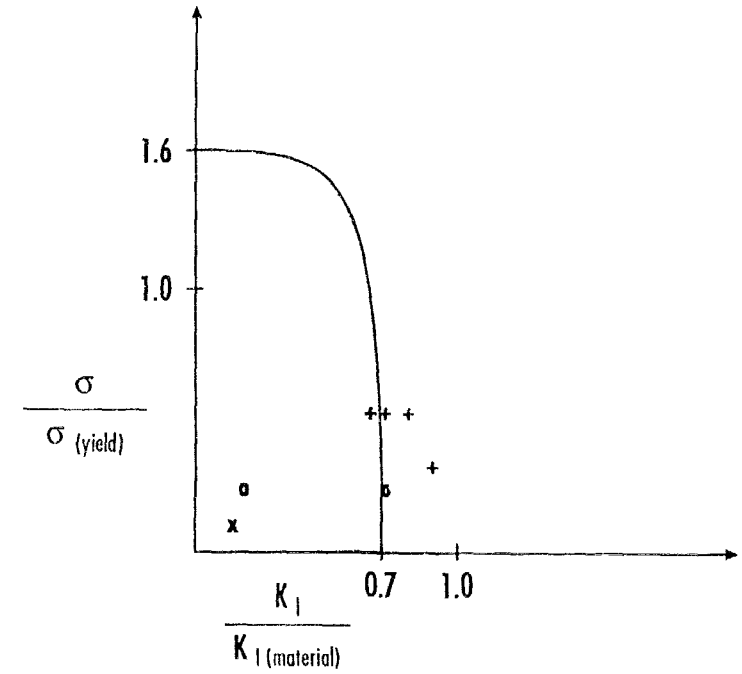

+ Results of four cask drop tests conducted at SNL
x Result of one cask drop test conducted at BAM
o Results of two cask drop tests conducted at CRIEPI

Note: Crack initiation did not occur in any of these drop tests.

(b)

FIG. 3.1 Failure assessment diagrams showing a conceptual view of tensile stress and fracture mechanics interaction (a) without safety factors and (b) with safety factors.

References

[3.1] SORENSON, K.B., et al., "Results of the Sandia National Laboratories MOSAIK Cask Drop Test Program", PATRAM '92 (Proc. Symp. Yokohama, 1992), Science and Technology Agency and Ministry of Transport, Tokyo (1993).

[3.2] GOLLIHER, K.G., WITT, C., WIESER, K., "Report on the Joint USA–Germany Drop Test Program for a Vitrified High Level Waste Cask", PATRAM '92 (Proc. Symp. Yokohama, 1992), Science and Technology Agency and Ministry of Transport, Tokyo (1993).

[3.3] ITO, C., et al., Research on Quality Assurance of Ductile Cast Iron Cask (Part 2), CRIEPI Rep. U91018, Central Research Institute of Electric Power Industry, Tokyo (1991).

Chapter 4

JUSTIFICATION OF SAFETY FACTORS

The safety margin concept

The risks represented by potential brittle fracture of materials used in the construction of radioactive material transport packages derive both from possible loss of containment of the radioactive material and from possible degradation of material used for radiological shielding or maintenance of subcriticality. These risks are mitigated, in large part, by the demonstration that the affected packaging materials can be used in a domain that is sufficiently remote from the domain in which the risk of brittle fracture might arise. It is the difference between the two domains which must be quantified, and this difference is commonly referred to as the safety margin.

The safety margin must always be adjusted to balance the severity of the consequences of brittle fracture (or any other potential failure mode) of the packaging materials against the economic penalties associated with preventing such failures. If the economic penalties are too great, operating constraints (e.g., weights or dimensions, fabrication costs, operating costs) may be prohibitive. On the other hand, the safety margin must be such that public health and safety is adequately protected.

For this reason, the concept of safety margin must be sufficiently robust to address the probability of occurrence of different loading events against the risk to the public health and safety associated with brittle fracture. The loading events may range from those to which the package will surely be subjected to extreme loading events that are unlikely to occur, but which are considered to be part of the design basis. In this case, the design basis includes the international criteria for certification of transport packages with their demonstration of satisfactory performance following a sequence of severe hypothetical thermal and mechanical loading events.

Experience from nuclear vessels and components

The preceding considerations imply safety margins that are balanced between the probability of occurrence of loadings events, the amount of risk that will be tolerated to the public health and safety, and the amount of investment risk represented by the temporary or permanent loss to the owner of the equipment. These can be combined and restated as the determination of the amount of damage that will be tolerated to the equipment, as a function of the probability of occurrence of the loading, and the determination of the associated safety margin. A conceptual basis for these determinations is provided by the ASME Boiler and Pressure Vessel Code, in particular Section III for nuclear power plant components [4.1]. Here the probability of occurrence of loadings are assigned to different levels, ranging from Level A (e.g., normal) to Level D (e.g., faulted) Service Conditions. Associated with each of these service levels is an overall description of the damage level to the equipment that will be tolerated. For example, the safety margins for Level A and Level B (e.g., upset) Service Conditions must be such that the component can continue to operate without interrupted service. Localized plastic deformation is permitted for components subjected to Level C (e.g., emergency) Service Conditions, and the component may require examination and possible repair prior to being allowed to resume operation following the loading event. Gross plastic deformation is permitted under Level D Service Conditions, and the component may have to

be replaced (and the owner's investment lost) in order to resume plant operation. Therefore, it is in the interest of both the equipment owner and the public to have safety margins that protect health and safety, while ensuring the continuing viability of the owner's investment.

In the case of radioactive material transport, the ASME approach would imply that normal conditions of transport should be covered with greater safety margins than the hypothetical accident conditions, since their probability of occurrence is high and the risk to both the public health and safety (and the owner's investment) should be essentially nil.

As an example of the determination of a safety coefficient for a particular failure mode in the ASME Code, consider the membrane stress plastic instability limit $P_m < S_m$, where P_m is the general primary membrane stress intensity calculated for expected design loading conditions and S_m is the allowable value for that stress intensity. S_m is derived from tensile test data, and is the lesser of 1/3 of the ultimate tensile strength or 2/3 of the yield strength. The former tends to govern the allowable for ferritic steels and the latter for austenitic stainless steels. As a result, the safety coefficient for ferritic steels for the plastic instability failure mode is 1/3 for expected loading conditions. The safety factor is 3.

The corresponding safety factor for Level D (e.g., faulted) Service Conditions depends upon whether elastic or elastic-plastic analysis methods are used to calculate the stresses [4.2]. In the former case, the allowable is 2.4 S_m. For the case of a ferritic steel with a minimum yield strength of 345 MPa and a minimum ultimate strength of 552 MPa, S_m would be 184 MPa and 2.4 S_m would be 441.6 MPa. If the ultimate strength defines failure, then the safety factor is 552/441.6 = 1.25. The safety coefficient is 0.80. Note, however, that the stresses calculated elastically are fictitiously high. In the case of stresses calculated elastic-plastically, the allowable is equal to the yield strength plus one-third the difference between the yield and ultimate strengths. For the ferritic steel example, this allowable would be 414 MPa, less than the elastic allowable; however, the calculated stresses more nearly represent reality. Assuming again that the ultimate strength defines failure, the safety factor is 1.33. The safety coefficient is 0.75.

At the present time, prevention of brittle fracture for nuclear power plant components is covered by a non-mandatory appendix (Appendix G) in the ASME Code [4.3], with limits on the general primary membrane stress under expected loading conditions provided in three ways: (1) a reference flaw must be postulated at the worst location and in the worst orientation with a depth equal to essentially 1/4 of the component wall thickness; (2) an explicit safety factor of 2 is applied to the general primary membrane stress; and (3) the allowable material fracture toughness is a lower bound of available data. The overall safety factor is not prescribed, but is at least 2 and actually much higher because of the conservatisms in the reference flaw and the material fracture toughness allowable. No guidance is provided in Appendix G for emergency or faulted loading conditions.

A more explicit assignment of safety factors is given in the ASME Code Section XI [4.4], which provides rules for the operation of nuclear power plant components. The rules for evaluation of detected and sized flaws found during in-service examination provide for safety factors to be applied to the material fracture toughness, as follows: (i) for normal conditions of loading, a safety factor of $\sqrt{10}$ (or about 3); (ii) for emergency and faulted loading conditions, a safety factor of $\sqrt{2}$ (or about 1.4). Note that these safety factors correspond closely to the safety factors given for plastic instability in Section III of the Code.

Application to transport safety margins

The normal conditions of transport against which transport packages must be designed correspond closely to the normal design loading conditions, and the regulatory tests relating to hypothetical accidents correspond closely to the faulted loading conditions of the ASME Code Section III. In the latter case, for example, the essential safety functions (i.e., containment, subcriticality and shielding) should be maintained, but on the basis of less stringent criteria (smaller safety coefficients) than for normal conditions; this would be in agreement with the regulations on authorized releases of radioactivity, which are greater for accident conditions than for normal conditions, as are dose rate limits [4.5].

Therefore, by analogy with ASME Code limits, it would be desirable to adopt an approach for brittle fracture prevention that is similar to the $P_m < S_m$ limit for plastic instability, taking the form

$$K_{I(applied)} < \frac{K_{I(material)}}{[safety\ factor]}, \tag{4.1}$$

where $K_{I(applied)}$ is the applied stress intensity factor and $K_{I(material)}$ is the material fracture toughness, in units of MPa $\sqrt{m}$. A similar relationship would apply for prevention of elastic-plastic fracture, if the methodology can be shown to be applicable. Equation (4.1) is analogous to $P_m < S_m$ in that the safety factor is applied to the right-hand side of the relationship (i.e., the property of the material) and the safety factor can vary with loading probability. Equation (4.1) can also be written as

$$K_{I(applied)} < \alpha\ K_{I(material)}, \tag{4.2}$$

where the safety coefficient $\alpha < 1$ and is adjusted for loading probability. Within the context of transport package brittle fracture evaluation, it is likely that the regulatory performance tests related to accidents dominate the evaluation process and that only the equivalent of Level D Service Conditions need be considered.

The appropriate safety factor (or safety coefficient) can best be determined by examining an expression for the applied stress intensity factor

$$K_{I(applied)} = C\sigma\sqrt{\pi a}. \tag{4.3}$$

In Eq. (4.3) it is crucial that the stress be determined with an adequate degree of accuracy and that the reference flaw be characterized in a conservative manner. The justification for the calculation of the stresses and the justification for the selection of the reference flaw size are covered in Chapters 7 and 5 of this document, respectively.

From these considerations, and by analogy with the safety factors and their reciprocal safety coefficients in the ASME Code Section III, a safety factor of three (or a safety coefficient of 1/3) is defendable for normal conditions and a safety factor of 1.4 (or a safety coefficient of 0.7) is defendable for the regulatory performance test conditions. Other margins may be justified by the package designer.

Parametric correction coefficients

The uncertainties which govern the selection of the safety factor for Eq. (4.1), or its reciprocal safety coefficient in Eq. (4.2), are related to the parameters in Eq. (4.3) and the material fracture toughness. In particular, the concern is the accuracy of the calculated or measured stress, the conservatism of the reference flaw, and the applicability of the measured fracture toughness data. For each of these quantities, depending on methodology, coefficients of correction can be used to guarantee the conservatism of assumptions or hypotheses that may be simplified or approximated. For example, the analytical representation of the reference flaw is that of a crack-like defect (infinitely-sharp crack tip radius) with a given shape, located at the most penalizing location (where the stress magnitude is greatest, usually at a surface), and in the most penalizing orientation (perpendicular to the direction of maximum stress). When testing is used to demonstrate margin against brittle fracture, the representation of the reference flaw requires consideration of each of these items. A somewhat deeper reference flaw may be required for such tests. The tip of the artificial flaw should be as crack-like as possible, or the effect of flaw sharpness on the characteristics of fracture toughness should be clarified.

Similarly, the stress calculations by package designers need to consider possible superposition of thermal and mechanical loadings, the conservatism and accuracy of dynamic or equivalent static stress analysis, material properties that may vary with strain rate, and many other factors. Again, some form of correction coefficient (e.g., a dynamic amplification factor) may be needed to assure the conservatism of the calculated stresses. If the stresses are inferred from strain and acceleration measurements in one or more tests, a similar evaluation of measurement accuracy must be addressed.

The remaining parameter in Eq. (4.3) is the form factor C, which is estimated using tables or obtained by direct calculation. In either case, it is necessary to assure that the factor used is representative of the actual geometry in question, or that some form of correction coefficient has been applied to assure conservatism.

Finally, the comparison of the calculated or measured $K_{I(applied)}$ to the appropriate material fracture toughness is of concern, as discussed in Chapter 6 of this document. Items to be considered include specimen thicknesses versus the packaging wall thickness, laboratory load application rates versus the loading rates of interest under the regulatory performance test conditions, and test temperatures versus those in the regulatory performance tests. If the demonstration is carried out by testing, there is an additional concern whether the material properties at the flaw location are representative of lower-bound material properties.

Appropriate correction factors will assure that the selected safety margin is defendable.

Elastic-plastic considerations

The governing Eqs (4.1) or (4.2) are valid only for conditions under which the plasticity at the tip of the flaw, and in the region around the flaw, is limited. For conditions of limited plastic deformation, an equivalent flaw depth can be used to account for the additional strain energy at the crack tip caused by the plastic deformation. Such corrections are usually small. If, on the other hand, the zone of plastic deformation in the region near the flaw becomes quite large, then the governing criterion is that of elastic-plastic fracture mechanics. Under these conditions, the justification for using elastic-plastic fracture mechanics techniques may be beneficial.

If elastic-plastic fracture mechanics techniques can be justified, the material property governing crack initiation is $J_{I(material)}$, rather than $K_{I(material)}$, and $J_{I(applied)}$ must be calculated, rather than $K_{I(applied)}$. Calculation of $J_{I(applied)}$ requires knowledge of the elastic-plastic properties of the material, including strain hardening information, and limit load calculations or measurements for the geometry under consideration. An extensive literature is available [4.6, 4.7].

When elastic-plastic fracture mechanics methods are used, the procedure for establishing the safety factor, or safety coefficient, is more complex. No longer is the safety factor reciprocal to the safety coefficient. In this case, the curve that represents the non-linear behaviour of the applied stress intensity factor, as a function of applied stress, must be known. Then, the point represented by the stress, as reduced by the safety factor (e.g., 1.4), should be located and the applied stress intensity factor at that point found. That applied stress intensity factor is denoted $J_{I(limit)}$. Then, the safety coefficient on J is defined to be $J_{I(material)}/J_{I(limit)}$.

References

[4.1] AMERICAN SOCIETY OF MECHANICAL ENGINEERS, Boiler and Pressure Vessel Code, Section III, Rules for Construction of Power Plant Components, Division 1, Subsection NB, Class 1 Components, 1989 Edition, ASME, New York (1989).

[4.2] AMERICAN SOCIETY OF MECHANICAL ENGINEERS, Boiler and Pressure Vessel Code, Section III, Nuclear Power Plant Components, Appendices, Division 1, Appendix F: Rules for Evaluation of Service Loadings with Level D Service Limits, 1989 Edition, ASME, New York (1989).

[4.3] AMERICAN SOCIETY OF MECHANICAL ENGINEERS, Boiler and Pressure Vessel Code, Section III, Nuclear Power Plant Components, Appendices, Division 1, Appendix G: Protection Against Nonductile Failure, 1989 Edition, ASME, New York (1989).

[4.4] AMERICAN SOCIETY OF MECHANICAL ENGINEERS, Boiler and Pressure Vessel Code, Section XI, Rules for In-service Inspection of Nuclear Power Plant Components, Subsection IWB: Requirements for Class 1 Components of Light-Water Cooled Power Plants, 1989 Edition, ASME, New York (1989).

[4.5] INTERNATIONAL ATOMIC ENERGY AGENCY, Regulations for the Safe Transport of Radioactive Material: 1985 Edition (As Amended 1990), Safety Series No. 6, IAEA, Vienna (1990).

[4.6] An Engineering Approach for Elastic-Plastic Fracture Analysis, Rep. EPRI-NP-1931, General Electric Company, Schenectady, NY (1981).

[4.7] DOWLING, A.R., TOWNLEY, C.H.A., The effect of defects on structural failure: A two-criteria approach, Int. J. Press. Vessels Piping **3** (1975) 77–107; and MILNE, I., AINSWORTH, R.A., DOWLING, A.R., STEWART, A.T., Assessment of the Integrity of Structures Containing Defects, Report R/H/R6-Rev 3, Central Electricity Generating Board, London (Original Report, 1976; Rev. 1, 1977; Rev. 2, 1980; Rev. 3, 1986); and MILNE, I. et al., Int. J. Press. Vessels Piping **32** (1988) 196.

Chapter 5

JUSTIFICATION OF REFERENCE FLAW SIZE

The use of a postulated or reference flaw to demonstrate the structural integrity of critical components is widespread in the nuclear industry. For example, Appendix G of Section III of the ASME Boiler and Pressure Vessel Code [5.1] provides for a reference flaw evaluation of ferritic pressure-retaining nuclear components through linear-elastic fracture mechanics procedures. Also, decisions on the frequency and extent of in-service examination can be based, in large part, on the results of flaw tolerance evaluations, an integral element of which is a reference flaw assumed to exist at a critical location in the component. An example of flaw tolerance evaluation is provided by the ASME Code Case N-481 [5.2]. In both of the examples cited, the depth of the reference flaw is required to be essentially one-quarter of the component thickness.

Similar procedures are applicable to the structural integrity evaluation of radioactive material transport packaging containment boundary materials, provided that the reference flaw characteristics can be justified in terms of industry design and pre-service inspection practices. The reference flaw size (i.e., depth and length) must be justified through three considerations: (1) the sensitivity of non-destructive examination detection and sizing; (2) the flaw size such that, if found during pre-service examination, would fail to meet quality assurance requirements (the rejection flaw size); and (3) the flaw size that would be potentially unstable under design-basis loading conditions (the critical flaw size). The relationship of the reference flaw to each of these "real" flaws is discussed in the following paragraphs.

Before addressing the detection and sizing of flaws, a rough idea of the number of flaws present in a typical packaging containment boundary is needed. For the purposes of this discussion, a flaw density of 6 flaws/m^3 is selected. This assumed flaw density is supported by the work of Harris and Lim [5.3], who recommended this value for steel weldments and forged plates, and by the Marshall report [5.4], which recommended a range of flaw densities from 0.4 to 40 flaws/m^3, depending upon particular quality control requirements. One widely-used probability density function for the distribution of existing flaw sizes is given by

$$P_a = \frac{\exp(-a/a_M)}{a_M[\,(1-\exp(\frac{-t}{a_M})\,]}, \tag{5.1}$$

where a = any flaw depth, t = the packaging wall thickness, and a_M is the mean flaw depth. Other expressions than Eq. (5.1) could be used for the probability density function that describes the distribution of existing flaw sizes. Equation (5.1) is sufficiently general to be used as an example of the relationship between real and reference flaws. For typical containment boundary wall thicknesses, where $t >> a_M$, this expression simplifies to

$$P_a = \frac{\exp(\frac{-a}{a_M})}{a_M}. \tag{5.2}$$

This expression can be integrated between appropriate limits in order to derive an expression for the probability of occurrence of flaws greater than a given size. For example, integrating between the depth a and an infinite flaw size gives

$$P_{>a} = \exp\left(\frac{-a}{a_M}\right) . \qquad (5.3)$$

This is the probability that a flaw of depth greater than a exists. If a_M is chosen to be 6.25 mm, then $P_{a(10\ mm)} = 0.197$. Therefore, for a package with a containment boundary volume of 11.5 m^3, with a total of some 70 flaws, about 13 (roughly one-in-five) flaws would have a depth greater than 10 mm. Furthermore, $P_{a(25\ mm)} = 0.017$, so that — for this same package — only one flaw with depth greater than 25 mm would exist.

In order to determine whether a mean flaw depth of 6.25 mm is meaningful, consider the flaw area that is cause for rejection of a ductile iron transport package in the Federal Republic of Germany, namely 50 cm^2. A semi-elliptic surface flaw of depth 31.75 mm, with a 6:1 aspect ratio, has an area of 47.5 cm^2, very close to this rejection flaw size limit. A semi-elliptic surface flaw of depth 32 mm, with the same aspect ratio, would have an area of 51.4 cm^2. If a_M were to be assumed to be 6.25 mm, then $P_{>a(31.75\ mm)}$ would be such that one out of every two packages of this type would have been rejected (assuming that these large flaws would have been found and sized correctly), which contradicts actual experience.

Suppose that a_M is chosen to be 3.8 mm. Then $P_{a(31.75\ mm)} = 2.4 \times 10^{-4}$, so that some 0.016 flaws of depth greater than 31.75 mm would exist, and about one out of every 62 packages would be rejected for service. Such a mean flaw size would imply very high quality casting, with few defects that would be grounds for rejection. If, instead, a_M is chosen to be 5.1 mm, then $P_{>a(31.75\ mm)} = 1.93 \times 10^{-3}$, so that 0.129 flaws of rejection size are present and one out of every eight packages would be rejected. Therefore, $a_M = 3.8$ mm represents high quality fabrication, $a_M = 5.1$ mm represents expected-quality fabrication, and $a_M = 6.25$ mm represents low quality fabrication.

Next, the reference flaw should be sufficiently greater in depth than a flaw with a 50% probability of detection (and adequate sizing) so that the detection and sizing of the reference flaw is virtually assured. In order to illustrate this point, suppose that an analytical formula is available that describes the detectability of flaws by non-destructive examination, and that this formula is given by

$$P_{ND} = 1/2\ erfc\ [\mu\ \ln(\frac{a}{a_D})] \qquad (5.4)$$

where P_{ND} is the probability of non-detection, *erfc* is the complementary error function, a_D is the flaw depth with a 50% probability of detection, a is any other flaw size, and μ is a parameter related to the standard deviation of the distribution; i.e., μ describes the variation in the detection or non-detection probability. If such a formula can be shown to be valid, then the probability of non-detection of any flaw can be estimated.

Comparison between the formula and actual non-destructive examination records show that $\mu = 1.0$ and $a_D = 10$ mm gives results that match well with actual experience. Then $P_{ND}(10\ mm) = 50\%$, of course, but $P_{ND}(15\ mm) = 28.5\%$ and $P_{ND}(25\ mm) = 9.75\%$. This means that about one out of every ten flaws of depth 25 mm or greater would go undetected. In order to have virtually assured detection, the reference flaw would have to be on the order of 40 mm in depth. In this case, $P_{ND}(40\ mm) = 2.5\%$ and only one out of every 40 flaws of depth 40 mm or greater would go undetected. If it could be demonstrated that a_D is 5 mm, rather than 10 mm, then $P_{ND}(40\ mm) = 0.2\%$; that is, only one out of every 500 flaws of depth 40 mm or greater would go undetected.

Results from the Plate Inspection Steering Committee (PISC) programme, an international effort aimed at the demonstration of volumetric examination capability [5.5], gives values for a_D as follows: 5 mm, for volumetric defects such as slag or lack of fusion; 12 mm, for defects with large, rough crack edges such as stress corrosion cracks or thermal fatigue cracks; and 28 mm, for defects with smooth crack edges such as vibration fatigue cracks. The Marshall report [5.4], which preceded much of the more advanced PISC work, surveyed in-service examiners and found that a_D was either about 6.35 mm or about 15 mm, depending upon whether the examiner was assessing his own performance or that of another examiner.

Recent progress in volumetric examination techniques is leading to lower a_D estimates. For example, a recent study carried out in Japan by the Central Research Institute of Electric Power Industry (CRIEPI) showed that blind ultrasonic examinations of calibration defects in thick ductile iron castings gave an a_D somewhere between 2.0 and 3.5 mm, with a very high probability of detection of calibration holes having diameters of 6 mm or smaller [5.6]. A related study carried out by the Electric Power Research Institute (EPRI) demonstrated that a_D is about 2.5 mm when modern ultrasonic examination and signal processing techniques are used [5.7].

Therefore, depending on the demonstrated quality of the volumetric examination, it can be seen that the reference flaw should be between four and eight times greater than the non-destructive examination detection and sizing sensitivity. This will virtually assure the detectability of the reference flaw. Somewhat lower depth values for the reference flaw could be justified by coupling volumetric with surface examination. Surface-breaking flaws represent a contribution to risk of package failure that is one to two orders of magnitude larger than that represented by embedded flaws, due to the higher stress intensity factors.

However, the probability of detection and adequate sizing is much better for surface flaws, especially if the surfaces are accessible for surface examination by dye penetrant, magnetic particle, or other inspection methods. The combination of a surface-breaking reference flaw and non-detection probabilities based on volumetric examination data produces a very high level of conservatism for the fracture mechanics evaluation approach.

The relationship of the reference flaw to the rejection flaw should be that the depth of the latter should be less than that of the former; i.e., the structural integrity evaluation procedure should be based on a reference flaw with a depth greater than that of the rejectable flaw size, in order to assure that the procedure is conservative relative to real flaws in the containment boundary. Of course, the rejection flaw size should be such that it has a high probability of detection and adequate sizing. Economical considerations will also dictate that the rejection flaw size should be as large as possible, consistent with protection of the public health and safety. Therefore, if the reference flaw depth is chosen to be 40 mm, a reasonable value for the rejection flaw depth is about 35 mm. Note that a 35 mm deep semi-elliptical flaw with a 6:1 aspect ratio has a plane area that is very close to 50 cm^2, which is — as stated previously — a current basis for rejection of ductile iron castings for transport packages. It is also worth noting that the probability of detection and sizing of such a real flaw is virtually assured, especially with a demonstrated detection sensitivity for volumetric examination of 5 mm or less, and with the added use of surface examination procedures in accessible locations.

The relationship between the reference flaw depth and the critical flaw depth is even less demanding. The critical flaw size should be greater than the reference flaw size, for obvious reasons. However, the margin between the two could range from a factor of two down to a factor of $\sqrt{2}$, depending upon the likelihood of the loading, without compromising the structural integrity process, since other conservatisms are applied to calculated stresses and to the margin required between $K_{I(applied)}$ and $K_{I(material)}$. (Safety margins are discussed in more detail in Chapter 4 of this document.) Therefore, if the reference flaw depth is chosen to be 40 mm, the fracture mechanics evaluation procedure would remain valid for critical flaw depths ranging upward from about 60 mm. A margin greater than two would be available for all critical flaw depths above 80 mm.

References

[5.1] AMERICAN SOCIETY OF MECHANICAL ENGINEERS, Boiler and Pressure Vessel Code, Protection Against Nonductile Failure, Appendix G, Section III, Division 1, ASME, New York (1989).

[5.2] AMERICAN SOCIETY OF MECHANICAL ENGINEERS, Alternative Examination Requirements for Cast Austenitic Pump Casings, Section XI, Division 1, Nuclear Code Case N-481, ASME, New York (1990).

[5.3] HARRIS, D.O., LIM, E.Y., Applications of a fracture mechanics model of structural reliability to the effects of seismic events on reactor piping, Prog. Nucl. Energy **10** (1982) 125–159.

[5.4] MARSHALL, W., An Assessment of the Integrity of PWR Pressure Vessels, Report of a Study Group, HM Stationery Office, London (1976).

[5.5] COWFER, C.D., "Basis/background for ASME Code Section XI proposed Appendix VIII: Ultrasonic examination performance demonstration", Nondestructive Evaluation: Planning and Application (Streit, R.D., Ed.), ASME, New York (1989) 1–5.

[5.6] IMAEDA, H., ARAI, T., ONCHI, T., On a Round Robin Test of Nodular Graphite Cast Iron Blocks by Ultrasonic Testing, CRIEPI Report No. T90059, Central Research Institute of Electric Power Industry, Tokyo (1991).

[5.7] WILLIAMS, R., "Ultrasonic inspection of ductile cast iron", paper presented at the 9th Joint Programme Committee Meeting, Tokyo, 1991.

Chapter 6

JUSTIFICATION OF MATERIAL FRACTURE TOUGHNESS

The increased activity in RAM shipping has resulted in an increase in new package design proposals. Candidate structural materials that have been proposed for packaging construction include ductile iron (DI), ferritic steel, titanium, borated stainless steel and depleted uranium. These structural materials may, when subjected to certain combinations of mechanical and environmental loadings, fail in a brittle fashion. Clearly, packagings constructed from these candidate materials must be evaluated properly to assure that brittle fracture will not occur.

Brittle fracture assessment techniques have been fragmented within the international RAM transport community. Although fracture mechanics is the fundamental engineering discipline that analyses fracture behaviour of solids, the historical lack of rigorous analysis and test techniques has limited the application in the RAM transport industry. In order to evaluate brittle fracture, industry and some competent authorities have substituted fracture mechanics analysis and testing with a variety of test procedures that provide a comparative measurement of impact absorption properties for metals with nominally similar compositions. Examples of these comparative types of tests include the Charpy V-notch, Drop Weight and Drop Weight Tear Tests. These test procedures can be categorized in general as notched impact tests and the results from these tests are used as a substitute measure for fracture toughness.

A major limitation of using these tests to evaluate brittle fracture is that they do not measure the appropriate material property; namely, fracture toughness. Knott [6.1] states: "The information obtained from notched impact tests cannot be applied directly to assess the resistance to fast crack propagation of a piece in service, because neither the fracture appearance nor the amount of energy absorbed can be related in a quantitative manner to the applied design stress, even if the geometry and strain rate associated with the impact test could be said to produce effects identical to those produced by service conditions. Impact-test information should really be used only to correlate with known performance in service. Provided that such correlations are made, the impact test provides comparative measurements of the toughness of different batches of steels of the same nominal composition, i.e., it may be used to give figures for quality control. Extensive correlations of this type have, however, been made for only a few specific applications". Since the notched impact tests measurements are not related to crack initiation behaviour, structural criteria related to notched impact properties tend to be overly conservative to the point of excluding candidate materials that may be suitable for a given application.

Additionally, the drop weight and the drop weight tear tests are specific to ferritic steels only. Therefore, brittle fracture evaluation criteria based on these test measurements exclude all other materials. Because of these limitations, a rigorous brittle fracture evaluation, based on fracture mechanics and fracture toughness testing, is established in this discussion. This approach is design based and is applicable to virtually any structural material.

The evolution of fracture mechanics analysis and testing has matured to the state that it can be used reliably for the design of structural components in RAM transport packages. The application of fracture mechanics design methodology (including the measurement of fracture toughness) has been accepted by the nuclear power plant industry. For example, the

American Society of Mechanical Engineers Boiler and Pressure Vessel Code (ASME B&PVC), Section III, Appendix G [6.2] and Section XI, Appendix A [6.3] both provide guidance for linear-elastic fracture mechanics evaluation. Other examples of fracture mechanics design methodology applied to the nuclear industry include Appendix ZG of the French Nuclear Code [6.4].

Adoption of the fracture mechanics design methodology and testing for the design of RAM transport packages has lagged behind the nuclear power plant industry. There are four basic items that have to be addressed in order to gain acceptance for this approach:

(1) using linear-elastic fracture mechanics criteria for elastic-plastic materials,
(2) effects of material inhomogeneity on fracture toughness,
(3) effects of dynamic loading rates on fracture toughness, and
(4) effects of section size on fracture toughness.

These four items are discussed in the following sections, with a summary of their current status.

In order to address these items, several international organizations involved in RAM transportation have had active research and development programmes directed at qualifying ferritic metals for structural use in RAM transport packages. Germany, Japan, France and the USA have all performed fracture toughness testing and verification cask drop testing to advance the fracture mechanics methodology. This work has focused on DI and justification for using fracture toughness measurements will be based on the DI work. However, the fracture mechanics analysis and fracture toughness testing is applicable to all structural materials. DI acts as a good benchmark material because it shows a ductile to brittle transition, as do most of the ferritic materials.

Using linear-elastic fracture mechanics criteria for elastic-plastic materials

Although the fracture mechanics methodology is applicable to all structural materials, fracture toughness measurements are based on two types of responses to loadings; either they respond in a linear-elastic (small-scale yield) fashion or they respond in an elastic-plastic (large-scale yield) fashion. There are two test procedures available for measuring fracture toughness based on the type of material response. ASTM E399 [6.5] measures plane-strain fracture toughness. K_{Ic}, the fracture toughness measurement obtained from E399, can be used directly as a design parameter. For many structural materials (including DI and ferritic steels), small-scale yield conditions cannot be met, and fracture toughness must be measured in accordance with ASTM E813 [6.6] or equivalent procedures, such as EGF-P1-90 [6.7]. This fracture toughness measurement, J_{Ic}, cannot be used directly in the linear-elastic analysis.

Therefore, the following conversion is used:

$$K_{Ic} = \sqrt{EJ_{Ic}}, \tag{6.1}$$

where E = elastic modulus (MPa).

This allows for linear-elastic fracture mechanics design methodology to be applied to an elastic-plastic material. Furthermore, demonstration drop tests (discussed in the section on size effects) indicate the conversion is conservative, provided that net section yielding does

not occur. The conservatism is further discussed and graphically shown in Chapter 3 of this document. Numerous drop test programmes have demonstrated the conservatism of this approach. Therefore, this item is not a topic for further research.

Effects of material inhomogeneity on fracture toughness

Organizations from Germany [6.8], Japan [6.9] and the USA [6.10, 6.11] have all conducted comprehensive testing of DI to characterize its mechanical properties (especially fracture toughness) as a function of composition, microstructure, loading rate, temperature, and section thickness. A DI database (which includes a large portion of the above data) has been compiled at Sandia National Laboratories [6.12]. For DI, the important attributes that control high fracture toughness are low pearlite and high sphericity of the graphite nodules. Additionally, given the preceding two conditions, fracture toughness increases with graphite nodule spacing. These data show that fracture toughness does vary with microstructure. However, a high quality ductile iron will respond in a ductile fashion.

Microstructure and composition can be controlled by using specification material. For example, ductile iron can be specified according to the German 1693 DIN (GGG-40), the ASTM A874, or the Japanese JIS G5504 specifications. These three specifications will produce the appropriate microstructure and composition that result in the high fracture toughness values for DI, and assure that production material will have mechanical properties representative of those of test programme materials.

Effects of dynamic loading rates on fracture toughness

The Japanese [6.13] and the USA [6.14] have conducted extensive dynamic rate fracture toughness testing on DI. For the loading conditions applicable to transport package criteria (i.e. a loading rate of approximately $\dot{K} = 10^3$ MPa$\sqrt{m}$/sec), fracture toughness values remain upper-shelf (ductile behaviour) and do not decrease appreciably relative to static measurements. This point has also been demonstrated in the MOSAIK Cask Drop Test Program [3.1]. A fifth drop test was made from a height of 18 m. This drop resulted in yield level stresses and, as predicted, crack initiation. Crack growth was arrested within one millimeter, indicating that the material was responding in the upper-shelf regime.

Work has also continued in improving dynamic rate fracture toughness testing capabilities. ASTM E813 does not provide procedures for dynamic rate testing. Salzbrenner [6.15] has developed a rigorous dynamic test compatible with E813 that results in upper-shelf behaviour at loading rates up to $\dot{K} = 10^4$ MPa$\sqrt{m}$/sec at -29°C. The importance of this work lies in the fact that the decrease in fracture toughness that has been found at dynamic rates using other test methods (i.e. pre-cracked Charpy tests) is in all probability due to the measurement techniques. The higher measurements corroborate with the results of the package drop tests. While further data may prove to be useful, the current description of dynamic loading rate effects is adequate.

Effects of section size on fracture toughness

Laboratory tests confirmed that DI responded in a ductile mode to mechanical loadings specified for transport packages (i.e., dynamic loadings at -40°C for a broad range of microstructures). However, scaling of the response of laboratory specimens up to full scale

packages had to be demonstrated. The Germans [6.16], Japanese [6.17] and the USA [6.18] have all published reports on drop test programmes that demonstrate that DI full scale packages will not fail in a brittle mode when designed using a linear-elastic fracture mechanics methodology. Further, these tests verify that laboratory tests can be used to measure material fracture toughness and to predict material response of a full scale package.

A secondary issue associated with transferring specimen tests results to full scale prototypes is that of notch acuity at the tip of the crack. ASTM E399 and E813 specimens are tested with fatigue cracks. This means that the radius at the tip of the fatigue crack approaches zero. Notches that are machined into packages for drop tests have crack tip radii that are relatively more blunt than the fatigue crack tip. The Japanese [6.13] have shown, for ductile iron, that a machined flaw with a crack tip radius ≤ 0.1 mm will produce fracture toughness measurements comparable with measurements obtained from specimens with fatigue flaws. Further the results of numerous drop tests demonstrate that the flaw tip radius in a drop test article is not a primary test parameter for ductile iron.

Other materials

DI was used as an example in this section because of the volume of R&D work that has been completed recently. Ferritic steels have been sufficiently characterized, and an extensive data base has been developed, such that the four items summarized in this chapter have largely been addressed. Minor issues regarding dynamic fracture toughness and section size effects continue to be studied. The maturity of the information on ferritic steels is reflected in the evaluation procedures of Section III, Appendix G, of the ASME Code.

Although this methodology has been shown to be applicable to transport package application using DI as a candidate material, any candidate material proposed for structural components in a packaging must have sufficient data to justify the discussed fracture toughness effects. The draft Appendix IX suggests a statistically significant database to justify the fracture toughness properties of the material and the design. More specific guidance is not warranted here since the requirements will vary based on the proposed material, the existing database, and the design. Draft Appendix IX of Safety Series No. 37 is written in a more general nature to reflect the application of all structural materials to the guidance given.

References

[6.1] KNOTT, J.F., Fundamentals of Fracture Mechanics, Butterworths, London (1973).

[6.2] AMERICAN SOCIETY OF MECHANICAL ENGINEERS, Boiler and Pressure Vessel Code, Section III, Nuclear Power Plant Components, Division 1, Appendix G, Protection Against Nonductile Failure, 1989 Edition, ASME, New York (1989).

[6.3] AMERICAN SOCIETY OF MECHANICAL ENGINEERS, Boiler and Pressure Vessel Code, Section XI, Rules for Inservice Inspection of Nuclear Power Plant Components, Appendix A, Analysis of Flaw Indications, 1989 Edition, ASME, New York (1989).

[6.4] French Nuclear Construction Code; RCCM: Design and Construction Rules for Mechanical Components of PWR Nuclear Islands, Subsection Z, Appendix ZG; Fast Fracture Resistance (1985).

[6.5] AMERICAN SOCIETY FOR TESTING AND MATERIALS, Standard Test Method for Plane-Strain Fracture Toughness of Metallic Materials, ASTM E 399, 1991 Annual Book of ASTM Standards, Vol. 03.01, Philadelphia, PA.

[6.6] AMERICAN SOCIETY FOR TESTING AND MATERIALS, Standard Test Method for J_{Ic}, A Measure of Fracture Toughness, ASTM E813, 1991 Annual Book of ASTM Standards, Vol. 03.01, Philadelphia, PA.

[6.7] EUROPEAN GROUP ON FRACTURE, Recommendation for determining the fracture resistance of ductile materials, Rep. EGF P1-90 (1989).

[6.8] GUNTHER, B., FRENZ, H., "Ductile cast iron (DCI) — Progress on research activities on fracture mechanics", PATRAM '89 (Proc. Symp. Washington, DC, 1989), Vol. II, Oak Ridge Natl Lab., TN(1989) 736–742.

[6.9] URABE, N., HARADA, Y. "Fracture toughness of heavy section ductile iron castings and safety assessment of cast casks", PATRAM '89 (Proc. Symp. Washington, DC, 1989), Vol. II, Oak Ridge Natl Lab., TN (1989) 743–752.

[6.10] SALZBRENNER, R., CRENSHAW, T., Mechanical Property Mapping of the Ductile Cast Iron MOSAIK KfK Cask, Sandia Report SAND90-0776, Sandia National Labs, Albuquerque, NM (1990).

[6.11] SALZBRENNER, R., Fracture toughness behaviour of ferritic ductile cast iron, J. Mater. Sci. **22** (1987) 2135–2147.

[6.12] McCONNELL, P., Ductile Iron Fracture Toughness Data Base, Sandia National Labs Contractor Report TTC-1057, under contract 66-1929 (1991).

[6.13] CENTRAL RESEARCH INSTITUTE OF ELECTRIC POWER INDUSTRY, Research on Quality Assurance of Ductile Cast Iron Casks, Rep. EL87001, CRIEPI, Tokyo (1988).

[6.14] SALZBRENNER, R., CRENSHAW, T., Multiple specimen J-integral testing at intermediate rates, submitted to Measurement Mechanics, 1988.

[6.15] SALZBRENNER, R., SORENSON, K., "Dynamic fracture toughness measurements of ferritic ductile cast iron", PATRAM '89 (Proc. Symp. Washington, DC, 1989), Vol. II, Oak Ridge Natl Lab., TN (1989) 728–735.

[6.16] WIESER, K., et al., "The status of ductile cast iron shipping and storage containers in the Federal Republic of Germany", PATRAM '89 (Proc. Symp. Washington, DC, 1989), Vol. II, Oak Ridge Natl Lab., TN (1989)701–711.

[6.17] KUSAKAWA, T., et al., "Full-scale tests and evaluation for quality assurance of ductile cast iron casks, PATRAM '89 (Proc. Symp. Washington, DC, 1989), Vol. II, Oak Ridge Natl Lab., TN (1989) 712–719.

[6.18] SORENSON, K., et al., "Results of the first thirty foot drop test of the MOSAIK KfK cask", Waste Management '91 (Proc. Conf. Tucson, 1991), Vol. 2 (1991) 707–713.

Chapter 7

JUSTIFICATION OF STRESS CONSIDERATIONS

When the potential for brittle fracture is evaluated by linear-elastic fracture mechanics methods, the fundamental condition for flaw initiation is given by the expression

$$K_{I(applied)} = K_{I(material)} . \tag{7.1}$$

The applied stress intensity factor can be determined from

$$K_{I(applied)} = C\sigma\sqrt{\pi a} . \tag{7.2}$$

As described in Chapter 4, uncertainty in the accuracy of calculated or indirectly-measured stresses is one of the reasons for applying safety factors to Eq. (7.1), such that the acceptance criterion for brittle fracture evaluation becomes

$$K_{I(applied)} < \frac{K_{I(material)}}{[safety\ factor]} . \tag{7.3}$$

Other reasons for the magnitude of the safety factor are the uncertainty in the flaw size or shape and uncertainty in material fracture toughness data.

Alternative procedures

Two different approaches can be used to determine the applied stress intensity factor, as shown in Fig. 7.1. First, the more conventional procedure is to calculate stresses, or measure strains in a test and infer stresses, or to calculate stresses and confirm their accuracy through comparison with test results. All of these options are shown as the top path in Fig. 7.1. Second, through the use of singularity functions, or calibrated test instrumentation, it is possible to directly determine the applied stress intensity factor, or to calculate the applied stress intensity factor and confirm its accuracy through testing. This approach is shown as the bottom path in Fig. 7.1.

A slight variation in both paths is to use scale-model test articles for the measurement of strains and the confirmation of stresses. In such a case, the principles of velocity scaling are used; that is, the equivalence of velocities (and stresses) between the scale-model and the full-scale test article is enforced, with the deformations and displacements scaled downward (by the scaling factor) and the decelerations scaled upward (by the scaling factor). The equivalence of velocities and stresses is enforced by using an equivalent loading (e.g., dropping the scale model from the same height as the full-scale test article). Significant strain rate effects undermine the equivalence, and applied stress intensity factors — as a combination of stress and dimension — do not scale properly. However, it is possible to use a flaw depth in the scale model that is greater than the flaw depth in the full-scale packaging, in order to enforce equivalence approximately.

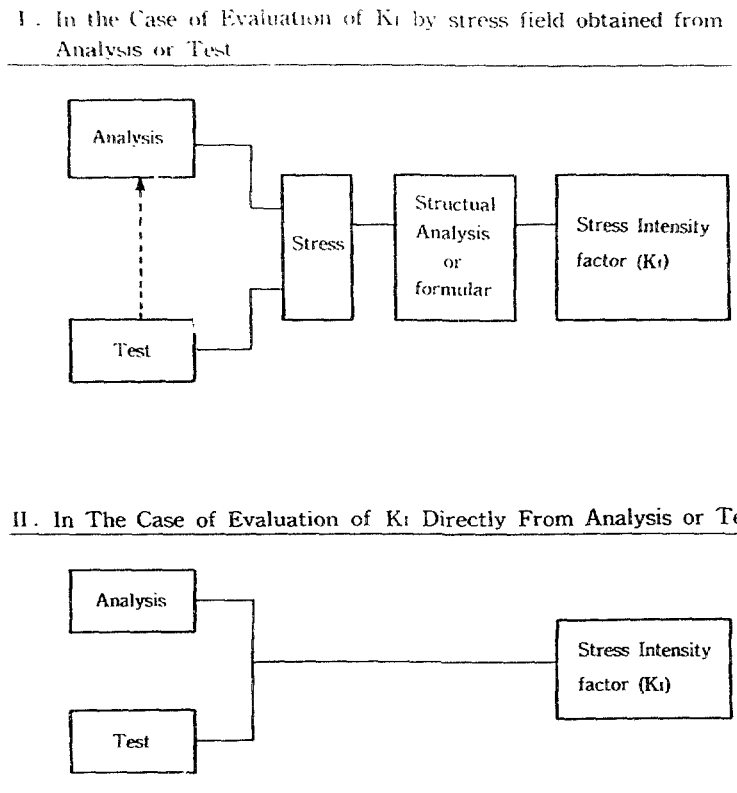

FIG. 7.1. Flow chart for evaluating the stress intensity factor.

Direct stress calculation

There are at least two possible direct analytical techniques for determining stresses caused by drop impact — one involving the calculation of stresses as a function of time by means of dynamic analysis, and the other by quasi-static analysis. The latter is based on decoupling the impact problem by assuming the shipping package to be modelled as one or more rigid masses, with steady decelerations for the rigid masses determined from the energy absorption characteristics of the attached impact-limiting devices. The steady decelerations are then applied as inertial forces on the packaging body, now treated as a deformable body, possibly with a dynamic amplification factor, in order to find the packaging body stresses. If the packaging body geometry is sufficiently simple, the stresses can be found from theoretical solutions of classical equations. Each of these two direct calculation methods is discussed in more detail below.

Dynamic analysis

Transport package drop impact analyses can be carried out using widely used finite element codes such as DYNA [7.1], HONDO [7.2] and PRONTO [7.3]. Considerable effort has been expended to verify the accuracy of these and other finite element and finite difference codes on impact problems [7.4–7.10]. A particular comparison between analyses and test results is shown in Fig. 7.2. The ratios of dynamically calculated versus experimental peak acceleration and strain vary considerably, but the scatter is such that an appropriate

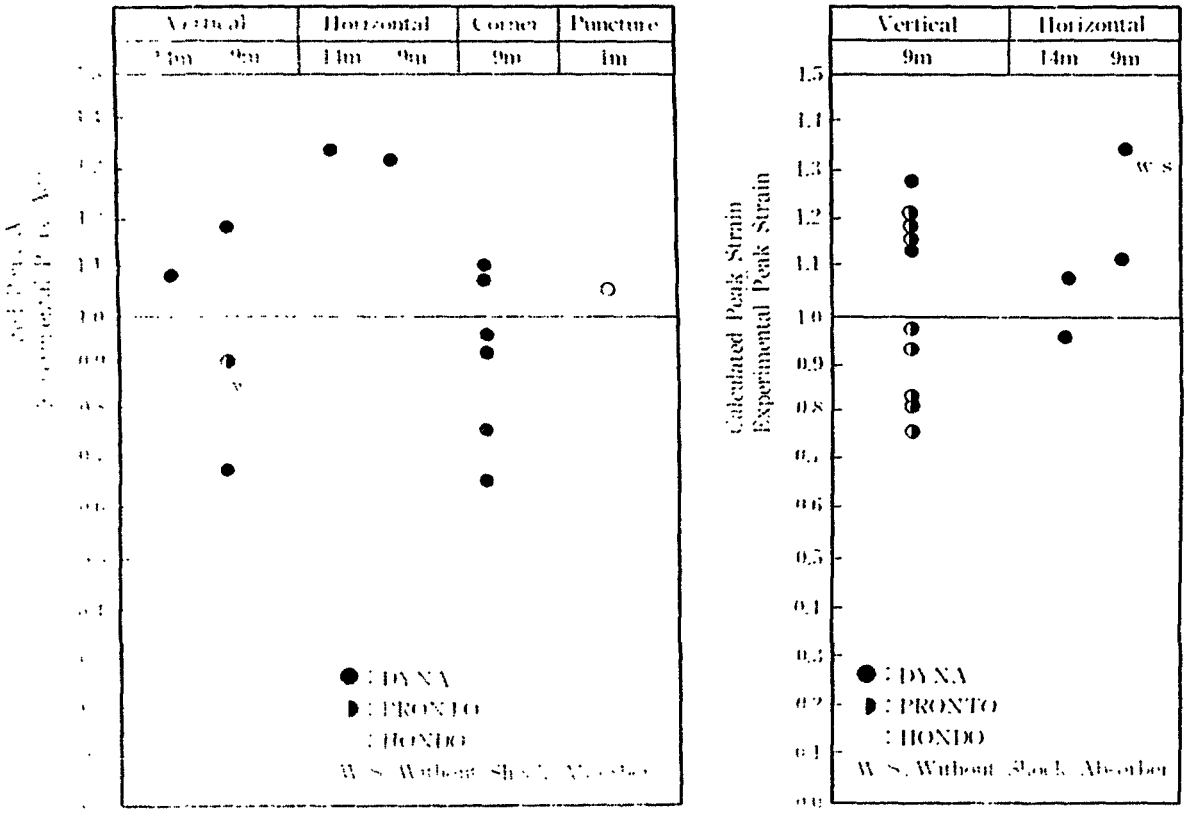

FIG. 7.2. Accuracy of dynamic analytical codes [7.4–7.11].

safety factor could be applied to Eq. (7.3) to treat the uncertainty. In order to improve the accuracy, modelling improvements are needed, particularly with respect to the material characteristics of the impact limiters. Programmes are under way to obtain the needed information [7.11–7.13]. Results from these programmes [7.14, 7.15]) have helped to clarify the differences between static and dynamic impact limiter properties, so that deformation rates can be accounted for in the dynamic calculations. Strain rate effects on mechanical properties may be of concern in modelling the packaging body components, as well.

The major considerations that need to be addressed when dynamically analyzing a transport package subject to drop impact are: (1) the approach used to integrate the discretized equations of motion, either explicit or implicit, and the numerical stability and accuracy of the methods; (2) any artificial damping inherent in the integration method or added to the calculation to control numerical "noise", and the effect of this artificial damping on interpretation of results; (3) any error controls built into the analytical software intended to provide more accuracy to the non-linear calculations, and the effect of these controls on convergence of the solution; and (4) the ability of the analytical software to accommodate load combinations, such as preloads in bolting and initial thermal stresses, in the impact calculations. Addressing these considerations becomes a part of the justification of the dynamic analysis procedure used.

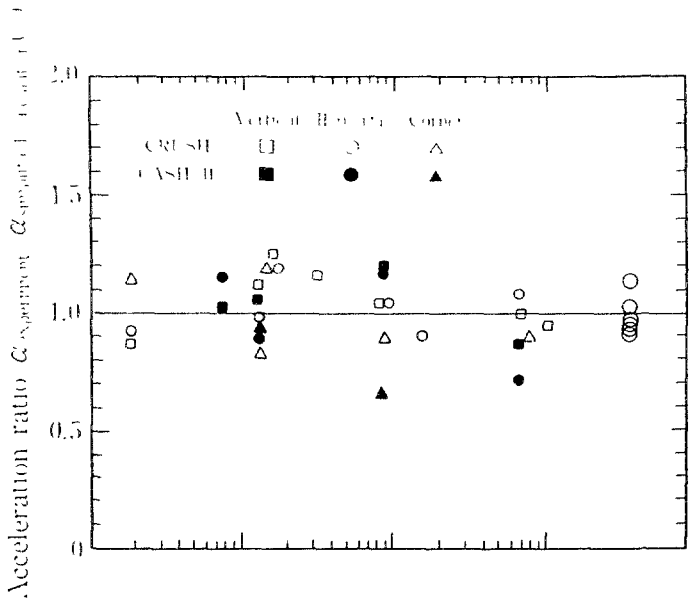

FIG. 7.3. Accuracy of the static analytical code.

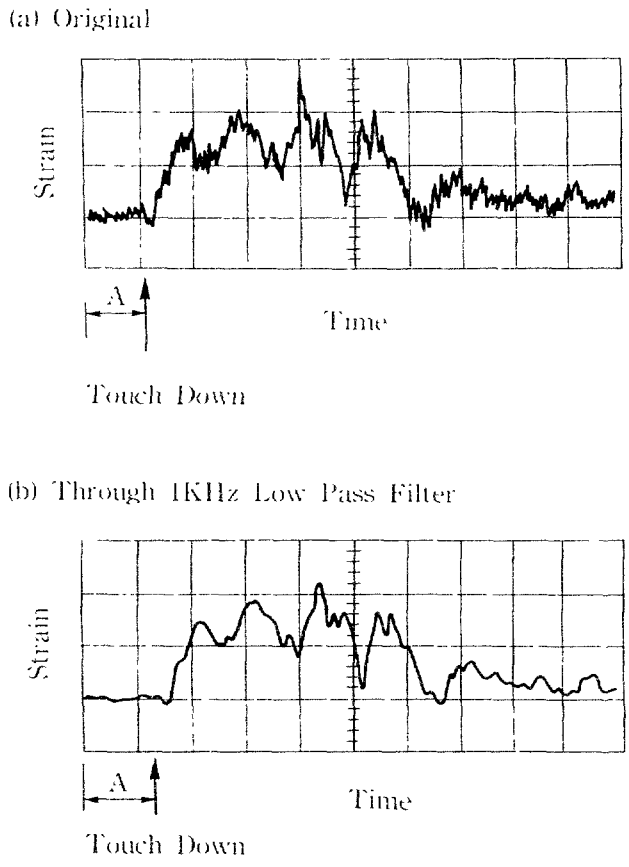

FIG. 7.4. Analysis of measured strain curve.

Quasi-static analysis

Quasi-static analysis methods can be used to determine the packaging body stresses directly also, provided that the response of the impact limiters and packaging body can be decoupled. This decoupling is based on the assumption that all of the impact energy is absorbed by the impact limiters, with the packaging body modelled as a rigid mass or a series of rigid masses. Then, after determining the steady decelerations from the decoupled analysis, the steady decelerations are applied to the packaging body, now treated as a deformable body [7.16]. It may be necessary to multiply the steady decelerations by a dynamic amplification factor in order to assure conservatism of the quasi-static calculations. The maximum value for such a dynamic amplification factor is two, but a more typical value (depending on the characteristics of the impact limiters) is 1.1 to 1.25.

Again, strain rate effects may be an important consideration. Typically, the decoupled analysis is carried out using dynamic loading properties of the impact limiter materials, while the quasi-static analysis usually involves strain-rate independent material properties for the packaging body. An example of a comparison between quasi-static calculations, using simplified analytical techniques, and test results is shown in Fig. 7.3. This comparison between test and calculated accelerations shows that a dynamic amplification factor (or a safety factor in Eq. (7.3)) of about 1.25 would be sufficient for accuracy verification.

Indirect stress calculation by test

For the indirect calculation of stresses from test results, the stresses are determined from strains obtained by attaching strain gauges to the packaging body at locations where maximum tensile stresses are expected to occur. The measured strain signal contains various amounts of noise resulting from the analog conversion of strain to an electronic waveform, in addition to the desired portion of the signal itself. Most of this noise is observed in a frequency range well above that represented by body deformation, corresponding to frequencies of 10 kHz and up, compared to body response in the tens and hundreds of Hz. This noise must be filtered out of the signal prior to any attempts to characterize the dynamic response. An example is described below.

An example of a dynamic strain waveform is shown in Fig. 7.4(a). The early-time portion of the signal (called Part A) occurs prior to impact, and any variation in the signal can be attributed to electronic noise. The low-pass filter conditioning system is applied to this portion of the waveform until the noise is eliminated. Then, this calibrated low-pass filter is applied to the signal over its entire range, leading to the filtered curve shown as Fig. 7.4(b). The remaining temporal variation in the smoothed signal presumably represents true dynamic response characteristics of the package.

Another potential pitfall is the interpretation of the dynamic response data in terms of the deceleration of the centre of gravity of the package and the packaging body vibrations. The smoothed strain signal contains both. If the intent of the data interpretation is to determine the deceleration of the centre of gravity of the package, methods are available to eliminate the body vibrations that are superimposed on the desired signal [7.18, 7.19]. A more serious concern is that the strain gauge locations may be at "nodes" of the body dynamic response, so that the dynamic amplification by body deformation is not accurately captured in the strain signals.

Another point of concern is that the strains are being measured only at the packaging body surfaces. Therefore, the associated stress distributions would usually be estimated by assuming a linear stress distribution across the packaging wall. Because the stress distributions for thick-walled packaging construction may not be linear, this approach may lead to an underestimation of the stress (see Fig. 7.5). Further, the presence of a membrane component of the stress may complicate the determination of the point in time at which the maximum tensile stress occurs (see Fig. 7.6). In this case, extreme values of surface strain need not correspond to the most extreme value of average (membrane) strain across the wall thickness. Evaluation of both extreme surface strain values and extreme membrane strain values is needed. For these reasons, a comparison of stress analysis results with measured strain results often assists in the interpretation of the more complete stress state.

Finally, strictly speaking, the effect of packaging body curvature on the measured strains and inferred stresses should be evaluated. Some efforts have been made to study this issue and determine its importance, with the result that the curvature is very nearly negligible, since the radius of curvature of the packaging body is large in comparison to the reference flaw dimensions.

Determining the applied stress intensity factor

After stresses have been calculated by either direct or indirect means, the applied stress intensity factor must be found and compared to the allowable in Eq. (7.3). Depending upon the orientation of the postulated or actual flaw in the packaging body, available analytical

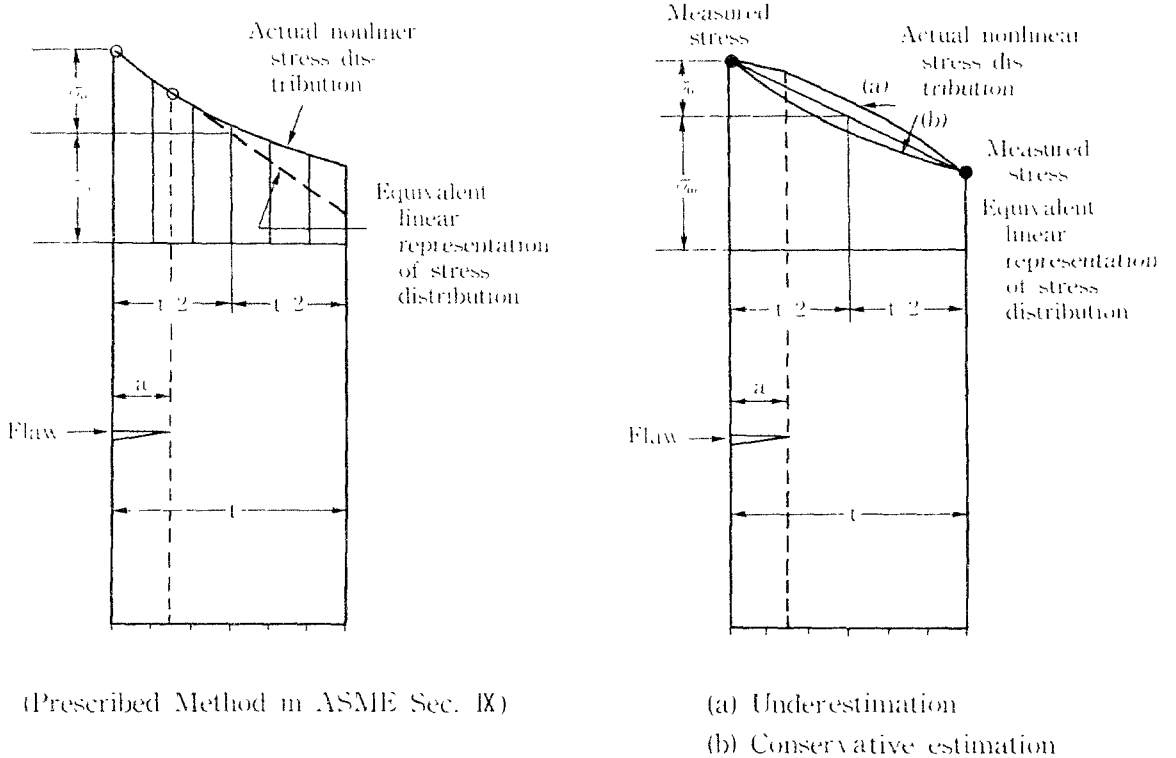

(Prescribed Method in ASME Sec. IX)

(a) Underestimation

(b) Conservative estimation

FIG. 7.5. Linearized representation of stress distributions.

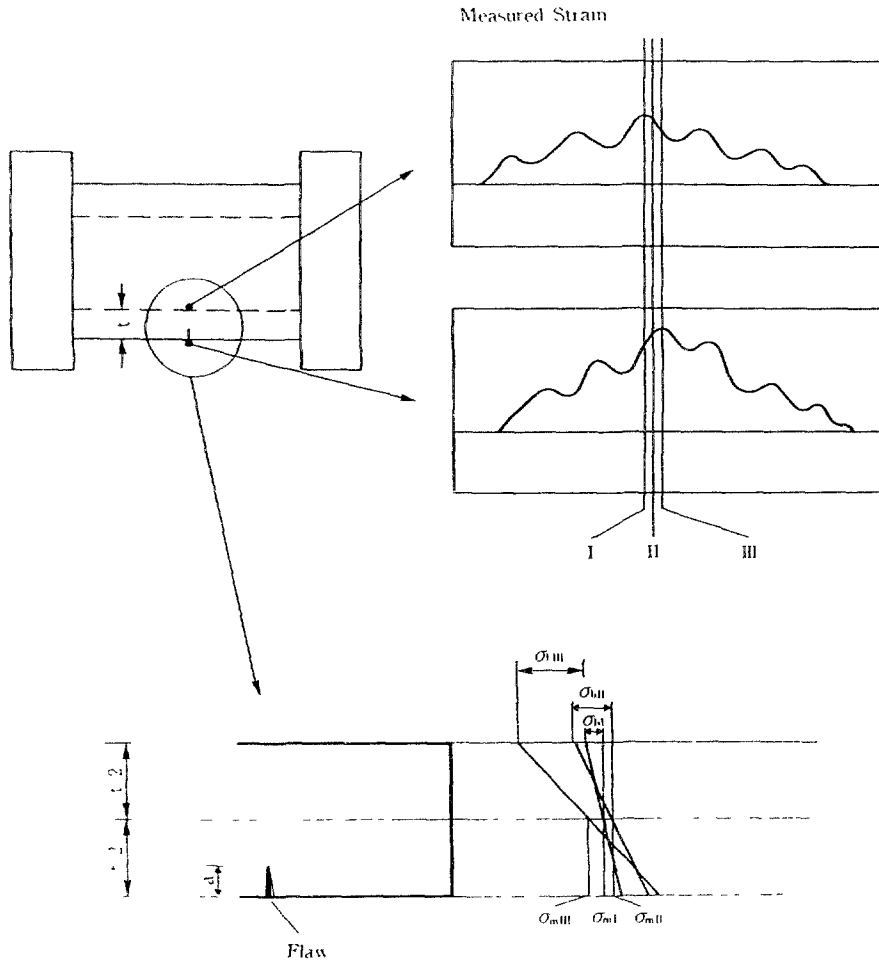

FIG. 7.6. Evaluation of stress distributions

results for two-dimensional cracks in well defined geometries, which are in the form of tables and simple formulas, may be used. For more complex shapes and flaw orientations, three-dimensional semi-elliptical surface crack results are available, such as those by Raju and Newman [7.20] and the method described in the ASME Code Section XI, Appendix A [7.21]. The latter has been widely used in nuclear power plant component flaw evaluation. Through tests on plate materials, it has been confirmed that this type of formula properly describes the crack initiation condition for ductile iron in a flawed package drop test [7.22].

In addition to the use of formulas and tables, the applied stress intensity factor can be found directly through the use of singularity finite elements or other means [7.23]. If this method is chosen, it is important to verify the accuracy of the direct calculation through some comparison with known solutions, in order to establish the convergence of the geometrical representation of the package and the type of loading.

References

[7.1] HALLQUIST, J.O., Theoretical Manual for DYNA 3D, Rep. UCID-19401, Lawrence Livermore National Lab., Livermore, CA (1983).

[7.2] KEY, S., HONDO: A Finite Element Computer Program for the Large Deformation Dynamic Response of Axisymmetric Solids, Rep. SLA-74-0039, Sandia National Labs, Albuquerque, NM (1975).

[7.3] TAYLOR, L.M., FLANAGAN, D.P., PRONTO-2D: A Two-Dimensional Transient Solid Dynamics Program, Rep. SAND86-0594, Sandia National Labs, Albuquerque, NM (1987).

[7.4] BUMPUS, S.E., GERHARD, M.A., HOVINGH, J., TRUMMER, D.J., WITTE, M.C., "Benchmarking of the computer code and the thirty foot side drop analysis for the Shippingport RPV/NST package", PATRAM '89 (Proc. Symp. Washington, DC, 1989), Oak Ridge Natl Lab., TN (1989).

[7.5] NEILSON, A.J., COOPER, C.A., BUTLER, N., "A programme to validate computer codes for container impact analysis", PATRAM '89 (Proc. Symp. Washington, DC, 1989), Oak Ridge Natl Lab., TN (1989).

[7.6] SAUVÉ, R.G., TULK, J.D., GAVIN, M.E., "Impact analysis and testing of tritiated heavy water transportation packages including hydrodynamic effects", PATRAM '89 (Proc. Symp. Washington, DC, 1989), Oak Ridge Natl Lab., TN (1989).

[7.7] SASAKI, T., KANAE, Y., SHIRAKURA, T., "The effect of secondary impact on a spent fuel shipping cask subjected to slant-angle drop tests", PATRAM '89 (Proc. Symp. Washington, DC, 1989), Oak Ridge Natl Lab., TN (1989).

[7.8] GEISER, H., HUEGGENBERG, R., RITTSCHER, D., "Experimental verification of dynamic stress analysis performed with DYNA 3D," PATRAM '89 (Proc. Symp. Washington, DC, 1989), Oak Ridge Natl Lab., TN (1989).

[7.9] GLASS, R.E., "Impact testing and analysis for structural code benchmarking", PATRAM '89 (Proc. Symp. Washington, DC, 1989), Oak Ridge Natl Lab., TN (1989).

[7.10] SAUVÉ, R.G., TEPER, W.W., SULLIVAN, G.J., "Material modelling and impact analysis of polyurethane foam filled T_2O transportation packages", PATRAM '86 (Proc. Symp. Davos, 1986), International Atomic Energy Agency , Vienna (1987).

[7.11] SHIRAI, K., ITO, C., Integrity of Cast-Iron Cask Against Free Drop Test (Part III), CRIEPI Rep. EU90001, Central Research Institute of Electric Power Industry, Tokyo (1990).

[7.12] AQUARO, D., FORASASSI, C., "Analysis of the behavior under impact loads of shell-type shock absorber for LWR spent fuel transport packaging", PATRAM '83 (Proc. Symp. New Orleans, 1983), Oak Ridge Natl Lab., TN (1983).

[7.13] WIESER, K.E., MASSLOWSKI, J.P., "Investigations on shock absorbers for Type B packagings", PATRAM '83 (Proc. Symp. New Orleans, 1983), Oak Ridge Natl Lab., TN (1983).

[7.14] SUGITA, Y., MOCHIZUKI, S., "The development of a toroidal shell-type shock absorber for an irradiated fuel shipping cask", PATRAM '83 (Proc. Symp. New Orleans, 1983), Oak Ridge Natl Lab., TN (1983).

[7.15] MEINERT, N.M., "Impact limiter design methodology", PATRAM '83 (Proc. Symp. New Orleans, 1983), Oak Ridge Natl Lab., TN (1983).

[7.16] IKUSHIMA, T., HODE, S., "Simplified analysis computer programs and their adequacy for radioactive materials shipping casks", PATRAM '89 (Proc. Symp. Washington, DC, 1989), Oak Ridge Natl Lab., TN (1989).

[7.17] ELECTRIC POWER RESEARCH INSTITUTE, Predrop Test Analysis of a Spent-Fuel Cask, Rep. EPRI-NP-4785, Palo Alto, CA (1986).
[7.18] WIESER, K.E., SCHUIZ-FORBERG, B., JAIS, M., "Acceleration and strain measurements performed on casks for radioactive materials under impact conditions", PATRAM '80 (Proc. Symp. Berlin (West)), Bundesanstalt für Materialprüfung, Berlin (West) (1980).
[7.19] YOSHIMURA, H.R., BATEMAN, V., CARNE, T.G., GREGORY, D.L., ATTAWAY, S.W., BRONOWSKI, D.R., "Force and moment reconstruction for a nuclear transportation cask using sum of weighted accelerations and deconvolution theory", PATRAM '89 (Proc. Symp. Washington, DC, 1989), Oak Ridge Natl Lab., TN (1989).
[7.20] RAJU, I.S., NEWMAN, J.C., Jr., Eng. Fract. Mechanics **11** (1979) 817.
[7.21] AMERICAN SOCIETY OF MECHANICAL ENGINEERS, Boiler and Pressure Vessel Code, Section XI, Rules for Inservice Inspection of Nuclear Power Plant Components, Appendix A, Analysis of Flaw Indications, 1989 Edition, ASME, New York (1989).
[7.22] ONCHI, T., KUSANAGI, H., SAEGUSA, K., Evaluation and Test on Brittle Failure Condition of Large DCI Plate, Central Research Institute of Electric Power Industry, Tokyo (1989).
[7.23] SHIRATORI, M., "Applications of FEM to Fracture Mechanics and Some Recent Topics," JSSC Vol. 22, No. 232 (1989).

LIST OF ABBREVIATIONS

ASME	American Society of Mechanical Engineers
ASTM	American Society of Testing and Materials
BAM	Bundesanstalt fuer Materialforschung und -pruefung (Germany)
B&PVC	Boiler and Pressure Vessel Code (ASME)
CRIEPI	Central Research Institute of Electric Power Industry (Japan)
DI	Ductile iron
DOT	Department of Transportation (USA)
EPRI	Electric Power Research Institute
J_I	Applied energy line integral (stress-strain field at the tip of a flaw) (N/m)
$J_{I(applied)}$	J_I and $J_{I(applied)}$ are used interchangeably in this text
$J_{I(material)}$	Material resistance to crack initiation under elastic-plastic conditions
$J_{I(limit)}$	Allowable applied J_I, with the appropriate safety factor considered
J_{Ic}	$J_{I(material)}$, measured at a static rate
K_I	Applied stress intensity factor at the tip of a flaw (MPa$\sqrt{m}$)
$K_{I(applied)}$	K_I and $K_{I(applied)}$ are used interchangeably in this text
$K_{I(material)}$	Material resistance to crack initiation under linear-elastic conditions
K_{Ic}	$K_{I(material)}$, measured at a static rate
K_{Id}	$K_{I(material)}$, measured at a dynamic rate
K_{Ib}	A lower-bound value of $K_{I(material)}$, selected from a statistically significant set of $K_{I(material)}$ measurements
NRC	Nuclear Regulatory Commission (USA)
NDTT	Nil-ductility transition temperature
NDE	Non-destructive examination
P_m	Primary membrane stress intensity calculated for the expected design loading conditions (MPa)
PISC	Plate Inspection Steering Committee
RAM	Radioactive material
S_m	Allowable stress intensity (MPa)
SAGSTRAM	Standing Advisory Group for the Safe Transport of Radioactive Materials (IAEA)
VHLW	Vitrified high level waste

CONTRIBUTORS TO DRAFTING AND REVIEW

Ershov, V.	All-Union Project and Scientific Research Institute, Russian Federation
Frenz, H.	Bundesanstalt für Materialforschung und -prüfung, Germany
Hirata, J.	International Atomic Energy Agency
Ito, C.	Abiko Research Laboratory, Japan
Mairs, J.H.	International Atomic Energy Agency
Moulin, D.	Commissariat à l'énergie atomique, France
Nickell, R.	Applied Science & Technology, United States of America
Pollog, T.	International Atomic Energy Agency
Selling, H.	International Atomic Energy Agency
Sorenson, K.	US Department of Energy, United States of America
Tanguy, L.	Commissariat à l'énergie atomique, France
Urabe, N.	Alloys & Corrosion Laboratory, Steel Research Center, Japan
Webster, T.	Department of Transport, United Kingdom
Wieser, K.	Bundesanstalt für Materialforschung und -prüfung, Germany